

**DEVELOPMENT AND APPLICATION OF LABVIEW PROGRAM
FOR ANALYSIS OF SOLAR CELLS
CURRENT-VOLTAGE DIODE PARAMETERS**

by
Mihir Malladi

A thesis submitted to the Faculty of the University of Delaware in partial fulfillment of the requirements for the degree of Master of Science in Electrical and Computer Engineering

Spring 2019

© 2019 Mihir Malladi
All Rights Reserved

**DEVELOPMENT AND APPLICATION OF LABVIEW PROGRAM
FOR ANALYSIS OF SOLAR CELLS
CURRENT-VOLTAGE DIODE PARAMETERS**

by

Mihir Malladi

Approved:

Steven S. Hegedus, Ph.D.
Professor in charge of thesis on behalf of the Advisory Committee

Approved:

Kenneth E. Barner, Ph.D.
Chair of the Department of Electrical and Computer Engineering

Approved:

Levi T. Thompson, Ph.D.
Dean of College of Engineering

Approved:

Douglas J. Doren, Ph.D.
Interim Vice Provost for Graduate and Professional Education

ACKNOWLEDGMENTS

It is my privilege to express the gratitude to all those who guided me in the completion of this thesis.

First, I would like to thank Dr. William Shafarman, Director of Institute of Energy Conversion for giving me an opportunity to work at the IEC. While working here I got a chance to work and interact with my advisor Dr Steven Hegedus and Research Associate Chris Thompson. I thank them for their patience and for their encouragement in completing this thesis work. I whole heartedly express my gratitude to them for giving me an opportunity to apply and further hone my skills in programming using LabVIEW software. The meetings we had while developing the program were very valuable. Their feedback and suggestions were so valuable that they not only helped me in improving my knowledge in photovoltaics and programming skills but also laid a foundation of an entrepreneur in me. It made me believe that customers know what they really want, and they are never wrong in most of the cases. I had worked on developing the program enthusiastically keeping this philosophy in mind.

I also would like to express my gratitude to my student colleagues at IEC: Nick Valdes, Alex Harding, Isaac Lam, Austin Kuba, Anish Soman, Sergio Sepulveda, Nuha Ahmed, Gowri Sriramagiri as well as fellow graduate student Abhishek Iyer for their valuable tips, discussions and suggestions in understanding the concepts related to photovoltaics, and how to survive as a graduate student.

Special thanks to Dr. Kevin Dobson, Abhishek Iyer, and Nuha Ahmed for giving their samples' data to analyze using my program.

Last but not the least I would dedicate this work to my parents for constantly supporting me and helping me persevere during difficult times and crisis situations.

Above all I thank the Almighty for his blessings to succeed in this effort.

TABLE OF CONTENTS

LIST OF TABLES	vii
LIST OF FIGURES	viii
ABSTRACT	xii

Chapter

1	INTRODUCTION	1
1.1	Understanding the functioning of a solar cell.....	1
1.2	Relevant Terms and Definitions	3
1.3	Outline of the Thesis	4
2	THE DIODE ANALYSIS	7
2.1	Method for performing the diode analysis	7
2.2	The Diode Parameters and their Importance	12
3	DEVELOPMENT OF LabVIEW PROGRAM FOR DIODE ANALYSIS	15
3.1	Brief Description about LabVIEW and its Significance	15
3.2	Benefits of Programming with LabVIEW.....	17
3.3	Why use a LabVIEW program for Diode Analysis?.....	17
3.4	DioMac Program and its Features.	19
3.5	Development of the Program and its Working.....	21
4	APPLICATION OF THE PROGRAM ON Cu(In,Ga)Se ₂ SOLAR CELL SAMPLES	31
4.1	Overview of the chapter	31
4.2	Cu(In,Ga) Se ₂ solar cells	31
4.3	Applying DioMac on CuInSe ₂ Sample at Different Temperatures	33
4.4	Application of Program on Cu(In,Ga)Se ₂ Solar Cells with High and Low FF	41
4.5	Applying Program in Analysis of an Anomalous Behavior of CIGS Solar Cell.....	45
4.6	Conclusions	46

5	APPLICATION OF THE PROGRAM ON SILICON SOLAR CELL SAMPLES	47
5.1	Overview of the chapter	47
5.2	Silicon Solar Cells Prepared in 2014.....	47
5.3	Silicon Solar Cells Prepared in 2018.....	49
5.4	Comparison of the diode parameter results for 2014 and 2018 samples.	51
5.5	Laser Fire Contact Silicon Solar Cells	57
5.6	Hybrid Silicon Solar Cells using PEDOT: PSS Polymer	60
6	CONCLUSIONS	62
	REFERENCES	64
Appendix		
A	FLOWCHART DIAGRAM FOR OBTAINING DERIVATIVES DJ/DV OR DV/DJ	66
A.1	Flowchart for numerical differentiation	66
B	FILES RELATED TO THE PROGRAM	70

LIST OF TABLES

Table 4.1	The Table containing the R2 values between analytical model and measured data under light and dark for CIS sample at different temperatures	41
Table 4.2	EDS and XRF Data for the CIGS samples having high and low fill factors	42
Table 4.3	Diode Parameters Results and Fill Factor correction under Light and Dark computed by DioMac for CIGS baseline run.....	44
Table 5.1	Tabulated diode parameter results of IBC and FHJ Silicon solar cell samples analyzed by DioMac.....	48
Table 5.2	Tabulated results of solar cell samples made in the year 2018 analyzed by DioMac.....	50
Table 5.3	Tabulated diode parameter results for the sample with cell ID MC 1690-04.....	58
Table 5.4	Tabulated diode parameter results for the sample with cell ID MC 1690-05.....	59

LIST OF FIGURES

Figure 1.1.	A brief overview of the basic functionality of solar cell [3].	2
Figure 1.2.	The equivalent circuit diagram of a solar cells.....	2
Figure 1.3.	The J-V characteristic curve of a solar cell under both Light (black) and Dark (red) conditions.....	4
Figure 2.1	The characteristic J-V curve of a CIS sample	8
Figure 2.2	Plot between dJ/dV vs Voltage under light and dark	9
Figure 2.3.	Plot between $(J+J_{sc})^{-1}$ and dV/dJ under light and dark conditions	10
Figure 2.4.	The semilogarithmic plot of $J+J_{sc}-GV$ vs $V-R_sJ$	11
Figure 2.5.	a) Influence of series resistance b) Influence of shunt and c) Influence of ideality factor on the J-V characteristics of solar cell and fill factor ..	13
Figure 3.1	An example of a front panel in LabVIEW: 1) Is the Front Panel window (Left) 2) Palette (right) containing controls and indicators for the front panel that perform input and output operations.....	16
Figure 3.2	Block diagram example. 1) Controls that act as source for data. 2)Indicators act as sinks, by collecting the result of an operation.....	17
Figure 3.3.	The front panel main menu window of DioMac. Comprises of four tabs: Main Window, J-V and Power Graph, File Details, Diode Parameters Results Tab.	19
Figure 3.4	Logo of DioMac program.....	20
Figure 3.5	The J-V curve under both Light and Dark conditions (to the left) and the power graph of J-V in light (to the right)	22
Figure 3.6	The flow diagram of DioMac depicting the working and flow of control.....	22

Figure 3.7	The front panel view of the second part of diode analysis under ‘ Light and Dark ’ conditions. Light data is in white color and the red is for Dark data.	25
Figure 3.8	The front panel view of the third part of diode analysis under ‘ Light and Dark ’ conditions. Light data is in white color and the red is for Dark data.	27
Figure 3.9.	Front panel view of the fourth part of the diode analysis. White plot is for the Light data and red plot is for the dark data.	29
Figure 3.10	Voltage correction plots for the light and dark data. White plot is for the original J-V curve, color red represents correction due to series resistance, blue for correction due to series and resistances, and yellow is for the dark data (due to J_{sc}).	29
Figure 4.1.	Schematic of a CIGS solar cell.....	32
Figure 4.2.	Analysis plots of the CIS solar cell sample at room temperature. a) The J-V curve b) dJ/dV vs Voltage c) dV/dJ vs $(J+J_{sc})^{-1}$ d) $\ln(J+J_{sc}-GV)$ vs $V-RJ$ e) J-V correction due to parasitic losses in light and dark f) Power vs Voltage graphs associated with the results in e)	34
Figure 4.3	Plots showing the comparison between the analytical model and measured data in light and dark at 25 Celsius.	34
Figure 4.4	Analysis plots of the CIS solar cell sample at 45 Celsius temperature. a) The J-V curve b) dJ/dV vs Voltage c) dV/dJ vs $(J+J_{sc})^{-1}$ d) $\ln(J+J_{sc}-GV)$ vs $V-RJ$ e) J-V correction due to parasitic losses in light and dark f) Power vs Voltage graphs associated with the results in e) ..	35
Figure 4.5	Plots of the analytical model and measured J-V data for the solar cell in light and dark under 45 Celsius temperature.....	36
Figure 4.6	Analysis plots of the CIS solar cell sample at -55 Celsius. a) The J-V curve b) dJ/dV vs Voltage c) dV/dJ vs $(J+J_{sc})^{-1}$ d) $\ln(J+J_{sc}-GV)$ vs $V-RJ$ e) J-V correction due to parasitic losses in light and dark f) Power vs Voltage graphs associated with the results in e)	37
Figure 4.7	The analytical model and the measured J-V data for the sample at temperature -55 Celsius.....	37

Figure 4.8	Analysis plots of the CIS solar cell sample at -75 Celsius. a) The J-V curve b) dJ/dV vs Voltage c) dV/dJ vs $(J+J_{sc})^{-1}$ d) $\ln(J+J_{sc}-GV)$ vs V-RJ e) J-V correction due to parasitic losses in light and dark f) Power vs Voltage graphs associated with the results in e)	38
Figure 4.9	Analytical model and measured J-V data under light and dark conditions for the CIS sample at -75 Celsius.	39
Figure 4.10	Analysis plots of the CIS solar cell sample at -105 Celsius. a) The J-V curve b) dJ/dV vs Voltage c) dV/dJ vs $(J+J_{sc})^{-1}$ d) $\ln(J+J_{sc}-GV)$ vs V-RJ e) J-V correction due to parasitic losses in light and dark f) Power vs Voltage graphs associated with the results in e)	40
Figure 4.11	The J-V analytical model and the measured current voltage data for the CIS sample at -105 Celsius light and dark.	40
Figure 4.12	An example of CIGS solar cell with high Fill Factor prepared by Dr. Kevin Dobson. a) The J-V curve b) plot dJ/dV vs Voltage c) dV/dJ vs $(J+J_{sc})^{-1}$ d) $\ln(J+J_{sc}-GV)$ vs V-RJ e) Voltage correction graphs in Light and Dark f) Power vs Voltage plot corresponding to plots in e) ...	43
Figure 4.13	An example of CIGS solar cells with low Fill Factor prepared by Dr. Kevin Dobson. a) The J-V curve b) plot dJ/dV vs Voltage c) dV/dJ vs $(J+J_{sc})^{-1}$ d) $\ln(J+J_{sc}-GV)$ vs V-RJ e) Correction of Voltages under Light and Dark due to parasitic losses. F) Corresponding Power vs Voltage plots.....	43
Figure 4.14	Example of a CIGS solar cell that does not follow the ideal diode model. a) J-V curve b) dJ/dV vs Voltage c) dV/dJ vs $(J+J_{sc})^{-1}$ d) $\ln(J+J_{sc}-GV)$ vs V-RJ e) Voltage correction in light and dark f) power vs voltages	45
Figure 5.1	Schematic of a standard Silicon Front Heterojunction Solar Cell [20]. ...	49
Figure 5.2	Plots representing the relationship between ideality factors under light and dark conditions. Plot (in left) are ideality factors calculated from part 3 and plot (in right) are ideality factors calculated from part 4 of diode analysis.	51
Figure 5.3	Plot showing the series resistance (light vs dark conditions) for 2014 and 2018 samples.	52
Figure 5.4	Plot of V_{ocq}/nkT vs $\ln(J_{sc}/J_0)$ under light and dark conditions respectively.....	53

Figure 5.5	J_0 current comparison under Light and Dark for 2014 and 2018 samples	54
Figure 5.6	Plots for Fill Factors vs Series Resistance in light a) Graph using the original fill factors b) Using Corrected Fill Factors c) Using the formula	55
Figure 5.7	Plots for Fill Factors vs Series Resistance in dark a) Using Corrected Fill Factors b) Using the formula of Martin Green	55
Figure 5.8	Plots for FF vs Ideality Factor a) Using Original Fill Factor b) Using Corrected Fill Factor c) Using the formula of Martin Green.	56
Figure 5.9	Plots for FF vs Ideality Factor in dark a) Corrected Fill Factor in dark b) Using Martin Green formula.....	57
Figure 5.10	Plots of the 3 rd part of diode analysis under light and dark for each week of observation.....	61
Figure A.1	Flow chart diagram representing the numerical differentiation done in computing the data for dJ/dV under part 2 of diode analysis. Same logic is applied in the 3 rd part for computing dV/dJ data.	68
Figure A.2	Block diagram in LabVIEW that performs the numerical differentiation under part 2 of diode analysis.....	69
Figure B.1	Screenshot of text file containing the calculated data while performing diode analysis.	71
Figure B.2	The tabulated results of the diode parameters computed for each sample loaded.	71
Figure B.3	Text file that keeps the record of the diode parameters for the samples run by the program	72

ABSTRACT

Photovoltaics is the technology that generates DC (direct current) electricity from semiconducting materials under the influence of light energy (photons). Solar energy has proven that human beings can get substantial portion of their electric power without dissipating non-renewable energy forms such as fossil fuels, thermal/nuclear, and coal.

The fundamental device used for developing PV systems is the solar cell. These solar cells comprise of semiconductor materials such as $\text{CuInGa}(\text{Se})_2$ (CIGS), Silicon (amorphous and polycrystalline), perovskites to name a few. Analysis of the current-voltage curve of the diode yields several parameters (called as diode parameters) such as series resistance, shunt resistance, ideality factor (also called diode quality factor), recombination current (J_0), and a correction to the Fill Factor due to series and shunt resistances. From these parameters one can understand the performance of the solar cell and how the photons are converted to electrons and how efficient these solar cells work. These parameters also allow conducting a loss analysis to determine dominant loss mechanisms and ultimate performance after removing the impact of these losses.

LabVIEW is a software developed by the National Instruments, that provides an environment for graphical computer programming. One can develop user-friendly programs not only for controlling for controlling instrumentation, operating control systems, data acquisition, but also as a tool for analyzing data.

In this thesis I have developed a program nicknamed as DioMac (short form of Diode Analysis Machine) which is a user-intuitive tool for performing the diode analysis technique and generating the diode parameter results that get stored in a text file. This will help the scientists/researchers to analyze the samples quickly and obtain accurate results. I have applied this program to analyze several solar cell devices made at the IEC from different materials (Silicon (front heterojunction (FHJ), using PEDOT:PSS polymer, interdigitated back contact (IBC)), Laser Fire Contact solar cells, $\text{CuInGa}(\text{Se})_2$, and $\text{CuIn}(\text{Se})_2$). The current vs voltage data were measured at IEC under light and dark conditions. For the CIGS solar cell samples, the current-voltage characteristics curves are measured and observed at various temperatures. For Silicon FHJ and IBC solar cell samples, the diode parameter results are generated, compared and the relationship between each other has also been observed. For silicon solar cells using PEDOT:PSS polymer stored under Nitrogen, degradation of the performance in each week has been observed. The current-voltage data (J-V) analyzed for most of the solar cells studied in this thesis were measured at room temperature but DioMac is easily applied to J-V curves obtained at different temperatures or light intensities as well. I found that it is easily applied to well behaved solar cell devices described by single diode model but cannot be applied to those with non-ideal cells with blocking barriers or voltage dependent current collection.

Chapter 1

INTRODUCTION

1.1 Understanding the functioning of a solar cell

Photovoltaic modules are the main components in power generation systems that harness solar energy. These photovoltaic modules are made of fundamental devices called solar cells [1]. The main steps involving in light to electricity conversion (as shown in Figure 1.1) are:

- 1) Absorption of light
- 2) Light-Carrier generation
- 3) Carrier Collection
- 4) Generation of voltage across solar cell
- 5) Losses in power due parasitic resistances [3][5].

These solar cells are made of semiconductors. The conversion of light (solar energy) to electrical energy occurs through photovoltaic effect [1]. The light energy conversion in a solar cell occurs in the form of a p-n junction [5]. The formation of the p-n junction diode is due to the junction between p-type and n-type semiconducting materials for example in a CIGS solar cell, the p-type is the CIGS while the n-type is CdS [2]. If photons entering the solar cell are absorbed, they create an electron-hole pair. The solar cell is a p-n junction that can be examined under two conditions: Light (with illumination) and Dark (without illumination).

Light Absorption + Carrier Generation + Carrier Collection

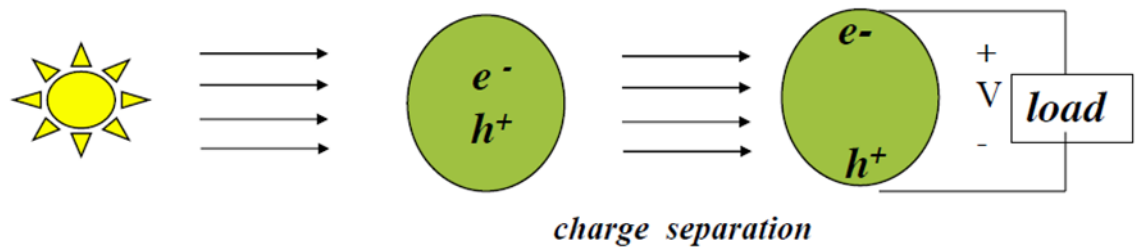


Figure 1.1. A brief overview of the basic functionality of solar cell [3].

Under the dark condition no light is incident on the solar cell and the diode behaves like a normal p-n junction. Under the light condition, when the light is incident on the solar cell a light dependent current is generated that is independent of the voltage [4]. The diode is in parallel with the light current source [3]. The equivalent circuit model is mentioned in Figure 1.2. This circuit diagram is a one-diode model.

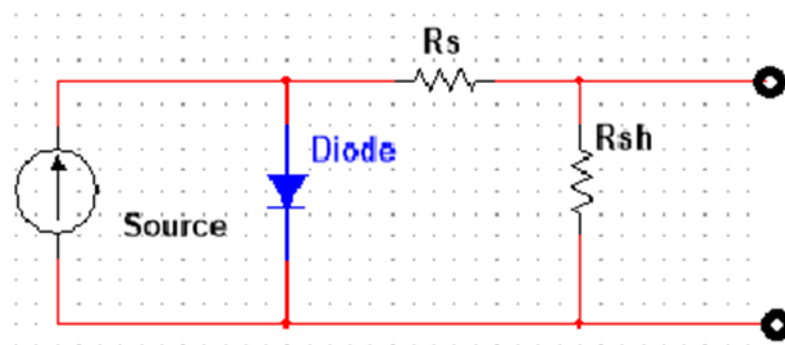


Figure 1.2. The equivalent circuit diagram of a solar cells

The lumped circuit model is as shown in Figure 1.2. The circuit comprises of the current source, the p-n junction diode, and the series and shunt resistances. The series resistance is due to the contact resistance between metals and other layers, by lateral sheet resistance in the transparent conductive oxide (TCO), and in the semiconductor (Silicon) [5]. The shunt resistance is due to defects and impurities that account for the power losses [6]. This equivalent circuit model in Figure 1.2 forms the basis for taking the current-voltage measurements and in performing the diode analysis. The current-voltage (J-V) measurements are taken using four-probe method using J-V tester and Oriel Simulator for illumination.

1.2 Relevant Terms and Definitions

Here are few definitions pertaining to the illuminated current-voltage characteristics of a solar cell with reference to J-V curve in Figure 1.3.

- 1) **Short Circuit Current (J_{sc}):** The short circuit current occurs when the voltage $V=0$. The unit for measurement is mA/cm^2 . This short circuit current depends on the bandgap of the semiconductor.
- 2) **Open Circuit Voltage (V_{oc}):** It occurs when current ($J=0$) hence there is no power. Referring to Figure 1.3 this occurs when the photocurrent or the light current $J_L=J_{sc}$. This parameter depends on the bandgap of the semiconductor. This parameter depends majorly on the recombination. The recombination losses limit the V_{oc} .
- 3) **Maximum Power Point:** It is the product of the maximum current (J_{max}) and maximum voltage (V_{max}).
- 4) **Fill Factor (FF):** It is the ratio of the product of the maximum power (product of V_{max} and J_{max}) over the product of V_{oc} and J_{sc} . This parameter is used to

understand the quality of a solar cell. It is influenced by the series resistance R_s , R_{sh} , and the diode reverse current J_0 [3].

$$FF = \frac{V_{max} * J_{max}}{V_{oc} * J_{sc}}$$

5) **Efficiency(η)**: It is the ratio of the maximum power to the input optical power of a solar cell.

$$\eta = \frac{V_{max} * J_{max}}{P_{in}}$$

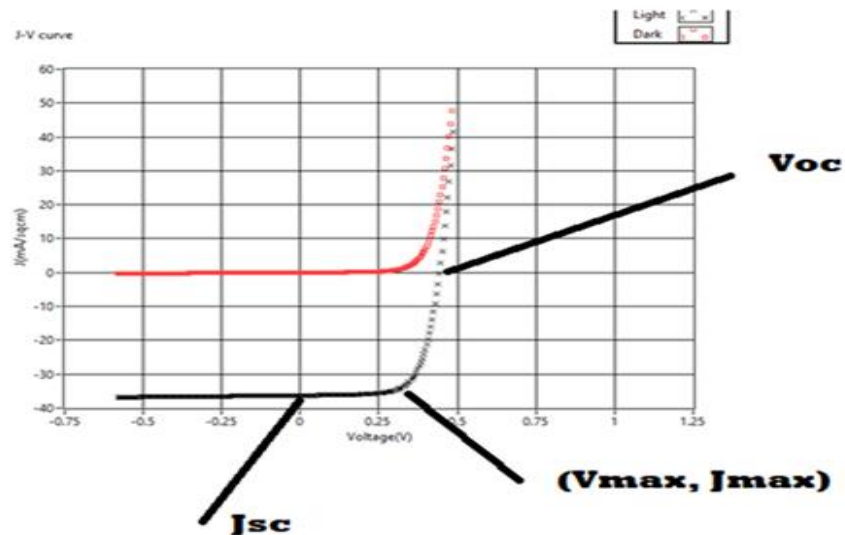


Figure 1.3. The J-V characteristic curve of a solar cell under both Light (black) and Dark (red) conditions.

1.3 Outline of the thesis

In this document the following information will be covered:

1) **Chapter 1:** In the first chapter a brief description about the operation of solar cell shall be discussed. This forms the basis for the diode analysis technique.

- 2) **Chapter 2:** In chapter two a detail description about the diode analysis technique will be covered, what parameters are obtained from it, and how these parameters contribute to various losses that affect the performance of a solar cell.
- 3) **Chapter 3:** A brief description about what LabVIEW is and why LabVIEW is used in developing a program for diode analysis shall be discussed. This chapter will give description about the functioning of DioMac (Diode Analysis Machine) program, the development of the program and the features of the program.
- 4) **Chapter 4:** In this chapter I shall discuss the application of the DioMac program on $\text{CuInGa}(\text{Se})_2$ solar cell samples. The program has been used to study the current-voltage characteristics under various temperatures of CuInSe_2 sample. This chapter will also describe the application of program on CIGS samples one having a high fill factor and other having a lower fill factor. The program has also been applied to a CIGS solar cell that shows anomalous behavior.
- 5) **Chapter 5:** This chapter will talk about the application of the program on Si solar cell samples. The performance of Interdigitated Back Contact (IBC), Front Heterojunction (FHJ) solar cells are discussed and their diode parameters are compared with each other. This chapter will also talk about the application of DioMac on the Laser Fire Contact solar cells. A brief discussion about applying the program on PEDOT: PSS polymer Si solar cell sample that is used for degradation study under nitrogen is also mentioned in this chapter.

6) Chapter 6: This chapter will talk about the conclusions and how DioMac can be used as a tool for diode analysis and help in studying the solar cells' behavior.

In the Appendix A I shall discuss the flow chart and block diagram to show the procedure/logic for developing a program snippet that performs numerical differentiation to obtain dJ/dV data and dV/dJ data (used in diode analysis). Appendix B will talk about the text files that are generated by DioMac.

THE DIODE ANALYSIS

2.1 Method for performing the diode analysis

From the equivalent circuit model in Figure 1.2, an equation is obtained that forms the basis of the solar cell analysis technique. This equation is called the **diode equation** that abides by the ideal diode law. The current-voltage behavior of the solar cells can be understood from this diode equation.

$$J = J_0 \exp\left[\frac{q}{AkT}(V - R_s J)\right] + GV - J_L \text{-----}(2.1)$$

Where R_s = Series Resistance

G_{sh} = Shunt Conductance

A = Ideality factor.

J_0 = Saturation Current Density

J_L = Light Current

Here we consider $J_L = J_{sc}$.

This assumption is true when the light current J_L is constant and independent of the voltage. However, this assumption is not valid in the cases where J_L depends on the voltage (voltage dependent collection $J_L(V)$). The voltage dependent collection is observed in thin film solar cells such as CuInSe₂, CdTe, and a-Si. The diode analysis comprises of four parts. Each of these parts comprise of a plot that determines one or

more of the diode parameters and compares them under both light and dark conditions. The paper in [7] written by Hegedus and Shafarman gives an elaborate explanation of the diode analysis technique. The four parts of the analysis are described below taking an example of a CuInSe₂ sample's measured J-V data.

Part 1: The first part is to obtain the standard J-V characteristic curve measured from reverse to forward bias in the light and in the dark, which is based on the equation in (2.1). From this J-V curve the **Fill Factor**, **Efficiency(η)**, **J_{sc}**, and **V_{oc}** are determined.

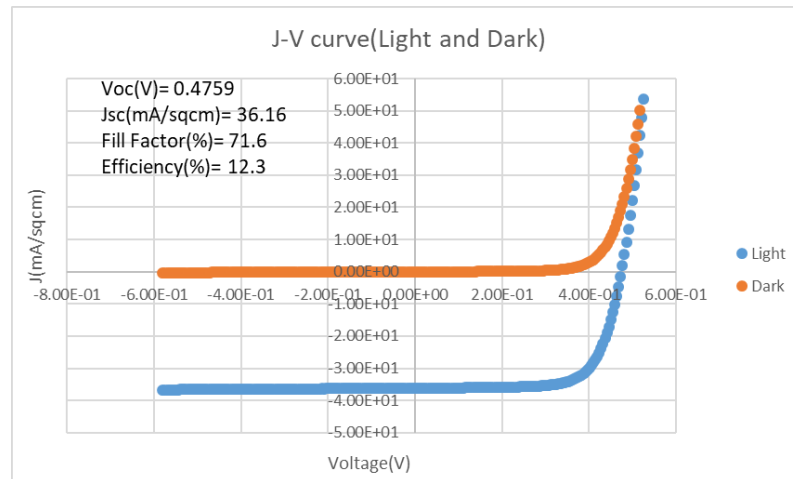


Figure 2.1 The characteristic J-V curve of a CIS sample

Part 2: The second part of the analysis is done by finding the derivative dJ/dV . Differentiating current density J in equation (2.1) with respect to the voltage (V) the **shunt conductance (G_{sh})** is obtained from the intercept of straight line fitted across the reverse bias region. The reciprocal of the shunt conductance gives the more commonly reported **shunt resistance (R_{sh})**. The dJ/dV data is plotted against the

Voltage and the curve is observed in the reverse biased region. A linear fit in this reverse biased region is used to determine the shunt conductance from the intercept. If the shunt term shows ohmic behavior and the light current J_L is constant, then the plot in the reverse biased region is flat [7] (generally observed in the dark). In light the plot in the reverse biased region is not flat and there is noise or oscillations.

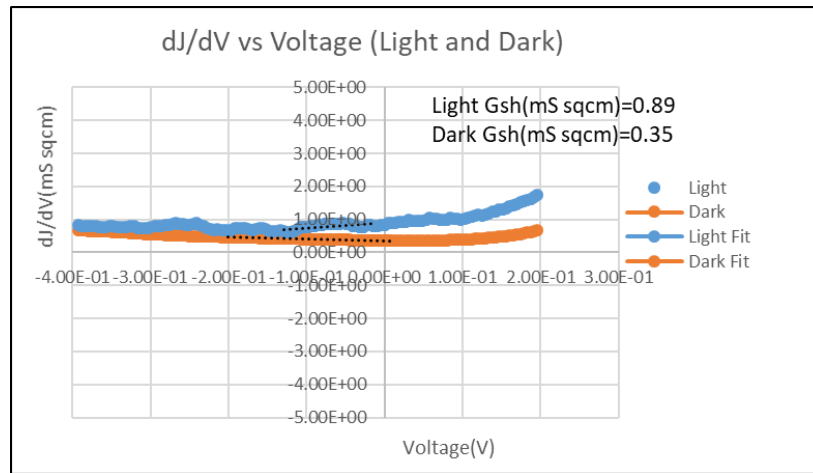


Figure 2.2 Plot between dJ/dV vs Voltage under light and dark

Part 3: In this part the analysis is done by finding the derivative dV/dJ . Here the equation (2.1) is differentiated with respect to the current density(J). The resultant equation will be:

$$\frac{dV}{dJ} - R_s = \left(\frac{AkT}{q}\right) (J + J_L)^{-1} \quad \text{-----(2.2)}$$

Equation (2.2) further can be further simplified as

$$\frac{dV}{dJ} = \left(\frac{AkT}{q}\right) (J + J_L)^{-1} + R_s \quad \text{-----(2.3)}$$

Assuming $J_L=J_{sc}$ the final equation will be

$$\frac{dV}{dJ} = \left(\frac{AkT}{q}\right) (J + J_{sc})^{-1} + R_s \quad \text{---(2.4)}$$

A plot between dV/dJ and $(J+J_{sc})^{-1}$ and a fit in the linear region of this data is used to determine the **series resistance(R_s)** and **ideality factor(A)** from the intercept and slope respectively. The straight line is because the light current J_L is independent of the voltage. There are cases where this plot shows a non-linear behavior. This non-linear behavior is due to presence of non ohmic contacts or due to a barrier in the current collection. This is called blocking behavior.

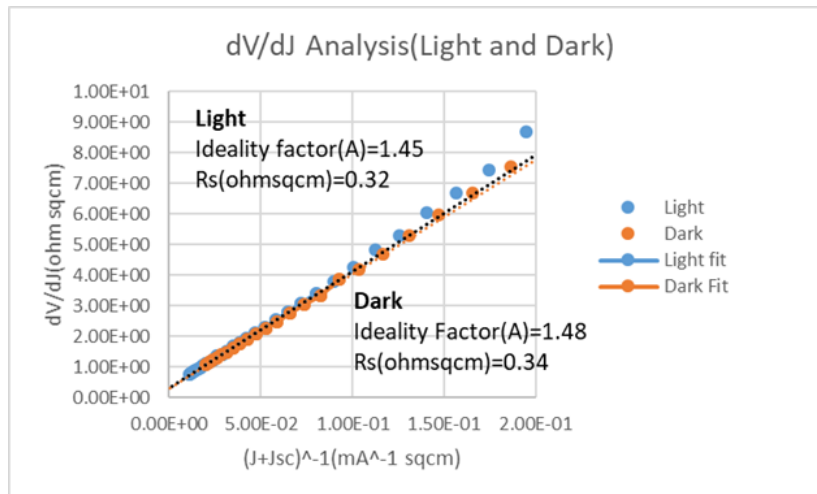


Figure 2.3. Plot between $(J+J_{sc})^{-1}$ and dV/dJ under light and dark conditions

Part 4: In part 4 a semilogarithmic graph of $\ln(J+J_{sc}-GV)$ vs $V-R_sJ$ is plotted. The $V-R_sJ$ data gives the correction in the voltage due to the series resistance while the term $J+J_{sc}-G_{sh}V$ gives the correction due to shunt. The correction of J-V curve for R_s and G_{sh} is required to identify the loss mechanisms and study the difference between the ideal behavior of a device and its actual behavior. Simplifying the diode equation in (2.1) taking the natural log on the LHS and RHS the following equation is obtained for Part 4.

$$\ln(J + J_{sc} - GV) = \ln(J_0) + \left(\frac{q}{AkT}\right)(V - R_sJ) \quad \text{-----(2.5)}$$

From the intercept and slope we obtain **J_0 current** and **ideality factor(A)** respectively.

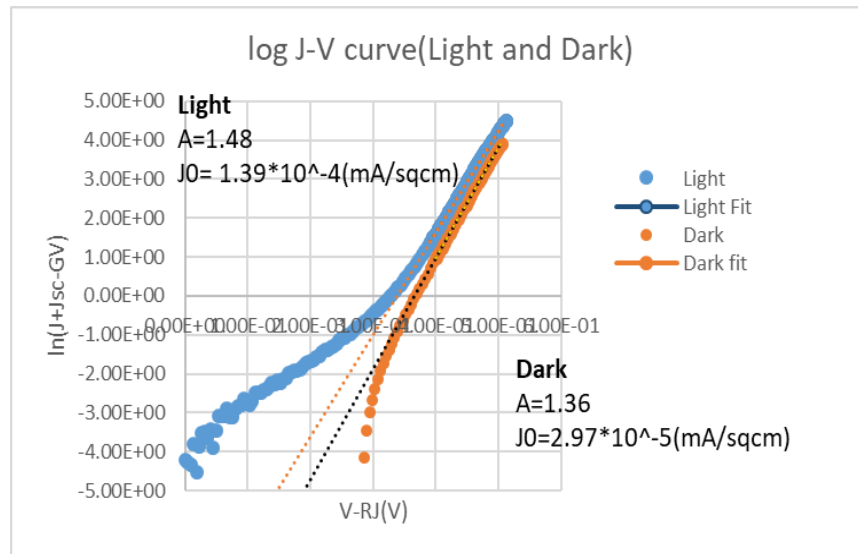


Figure 2.4. The semilogarithmic plot of $J+J_{sc}-GV$ vs $V-R_sJ$.

2.2 The Diode Parameters and their Importance

The diode parameters obtained from the four parts of the analysis are as described below:

- 1) **Series Resistance(R_s)**: The series resistance lumps together all resistance components whether due to lateral or vertical current flow. Examples include contact resistance between metal and semiconductor, resistance between ITO and metal grid contacts, and due to the bulk of the cell (bulk resistance) [2][6].
- 2) **Shunt Resistance(R_{sh})**: The shunt resistance is due to defects and impurities but also due to direct pathways for current between the front and back contact which bypass the junction [5]. The shunt resistance occurs parallel to the diode in the circuit diagram. The series and shunt resistances are parasitic losses and they have an impact on the Fill Factor and Figure 2.5 b) and c) show the influence of these parameters in the J-V characteristics.
- 3) **Ideality Factor(A)**: It is also called as the diode quality factor. It is a factor from which one can determine the quality of a solar cell. It typically has a value ranging between 1 and 2. The ideality factor causes a reduction in the Fill Factor [8] as shown in Figure 2.5(c). When A is approximately equal to 1 it means there is band-to-band recombination in the quasi-neutral region and when it tends to 2 it means there is defect-related recombination in the space charge region [9]. Here we are assuming a single p-n junction diode model for the analysis. However, some of the solar cells have a two-diode model with $A=1$ and $A=2$.

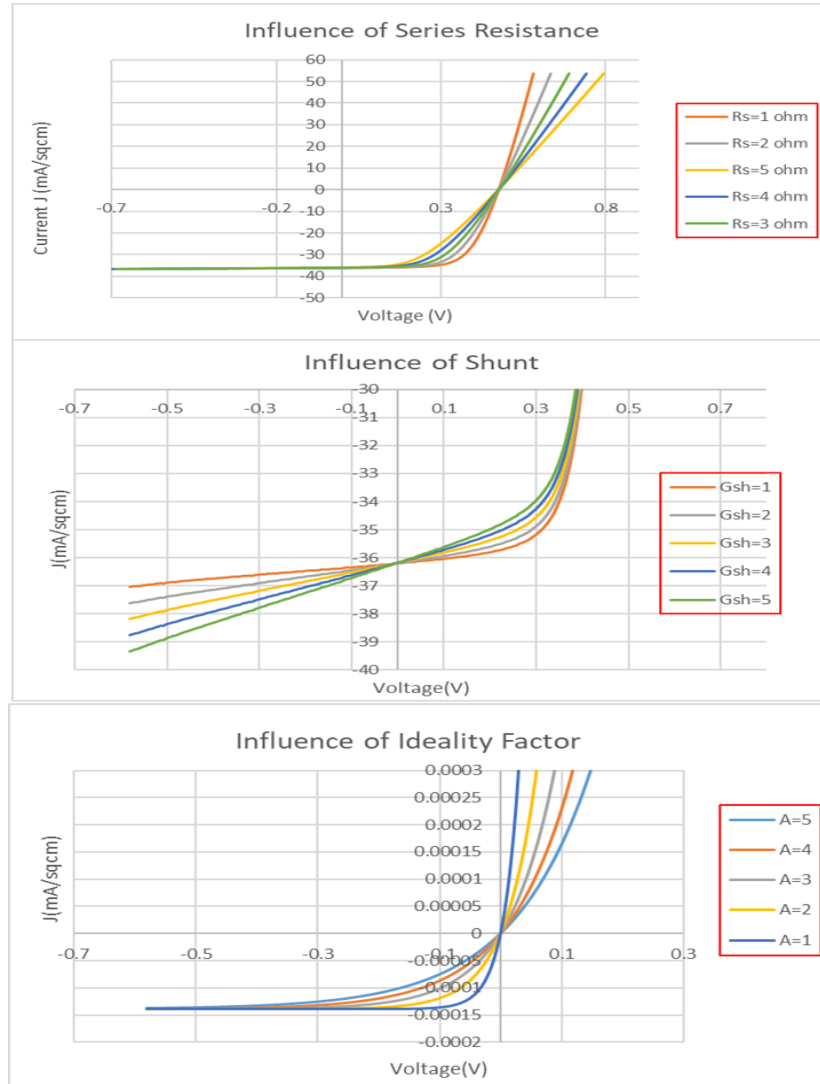


Figure 2.5. a) Influence of series resistance b) Influence of shunt and c) Influence of ideality factor on the J-V characteristics of solar cell and fill factor

4) **Saturation Current Density(J₀)**: It is given by the equation:

$$J_0 = J_{00} \exp\left(-\frac{\phi_b}{AkT}\right) \quad \text{-----(2.6)}$$

Where ϕ_b is the barrier height and J_{00} is the prefactor current. This prefactor saturation current depends on various recombination mechanisms that influence J_0 . As seen above, J_0 is governed both by recombination (J_{00}) and activation of carriers over a barrier. From these parameters one can determine the recombination mechanism that has impact on the V_{oc} [7]. The equation for V_{oc} is given by:

$$V_{oc} = \frac{\phi_b}{q} - \frac{AkT}{q} \ln\left(\frac{J_{00}}{J_L}\right) \text{-----}(2.7)$$

DEVELOPMENT OF LabVIEW PROGRAM FOR DIODE ANALYSIS

3.1 Brief Description about LabVIEW and its Significance

LabVIEW stands for Laboratory Virtual Instrumentation Engineering Workbench. It is an environment developed by National Instruments (NI) for visual programming. It is one of the primary choices in designing control and analysis solutions in engineering [10]. It is based on the concept of Virtual Instrumentation (VI), which is an interdisciplinary field that merges sensing, hardware and software technologies for creating intuitive applications that are used for controlling and monitoring [11]. Here the programs are coded by using graphical icons that have a specific function such as storing data as an array, performing basic arithmetic and logical operations, statistics, and several other functions related to math and engineering. LabVIEW is a strong tool used for building programs that perform operations such as instrumentation, automation, data acquisition, measurement and analysis, controlling and monitoring systems, processing of signals, and making real-time embedded systems. LabVIEW consists of two windows: The Front Panel and The Block Diagram Window. The Front Panel is used for observing output and acts as an interface between user and the program [12]. The block diagram window is used for developing the programs by connecting blocks/icons using wires. The data types of each graphical icon and block is determined based on its color. For example, if the color is in orange then the data-type is float/fractional decimal, if blue it is of integer type, green for Boolean type. An example of front panel and block diagram is shown

in Figures 3.1 and 3.2 respectively. This is an example of a basic 4:1 multiplexer, a device that combines four input lines and outputs a single line. Multiplexers are generally used in networking and telecommunication systems.

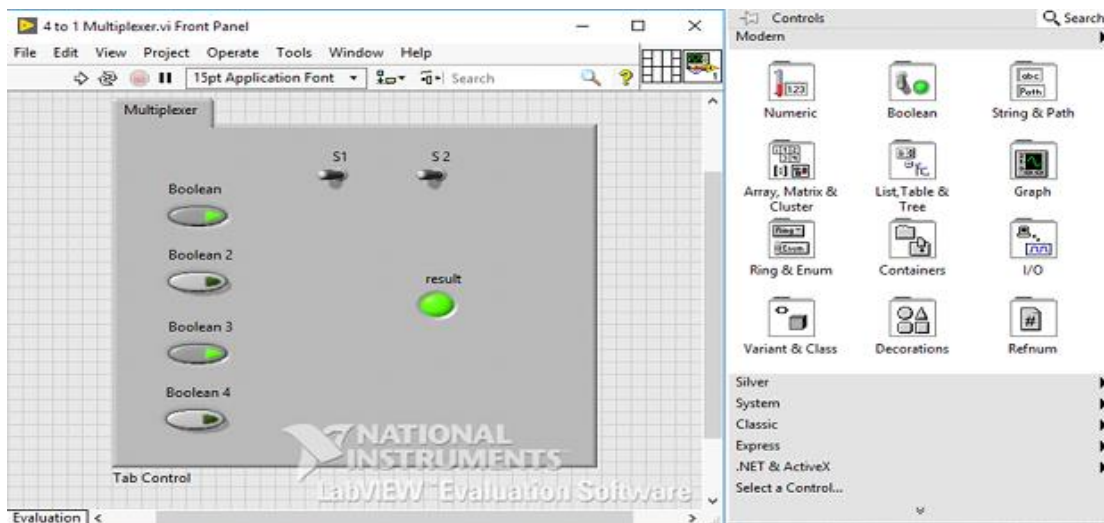


Figure 3.1 An example of a front panel in LabVIEW: 1) Is the Front Panel window (Left) 2) Palette (right) containing controls and indicators for the front panel that perform input and output operations.

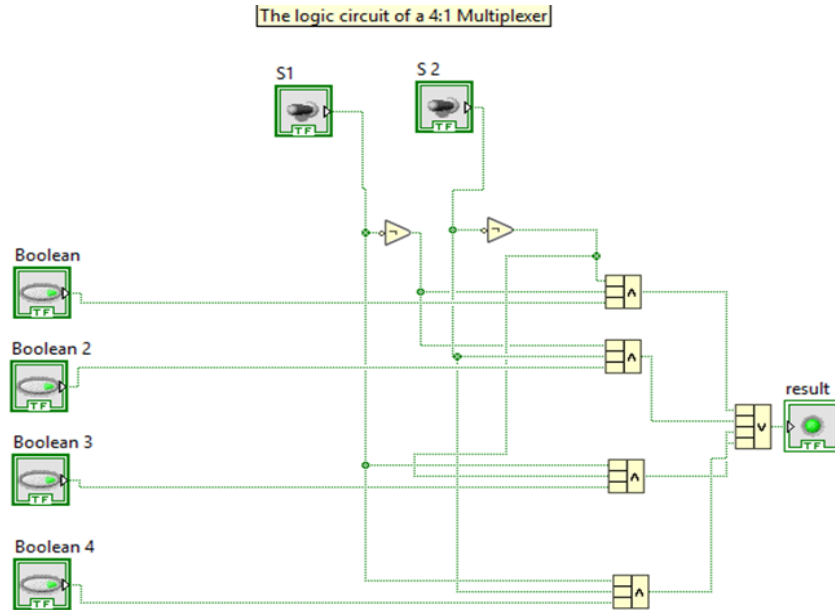


Figure 3.2 Block diagram example. 1) Controls that act as source for data.
2) Indicators act as sinks, by collecting the result of an operation.

3.2 Benefits of Programming with LabVIEW

LabVIEW provides intuitive graphical programming. The code used in LabVIEW environment is G-code. It enables scientists and engineers to visualize and model processes and tasks diagrammatically using the block diagrams and icons [13]. It is easy to compile and debug error in the codes by observing the run button on the front panel. Another advantage of LabVIEW is that one can solve mathematical problems and the program made in LabVIEW can also be combined with other programming languages.

3.3 Why use a LabVIEW program for Diode Analysis?

For performing diode analysis at IEC, we generally use Microsoft Excel or Origin, where one does calculations and linear fits on the data. However, Excel and Origin have several drawbacks. In Excel one analyses samples' data manually and

must plot the curves for each part, change the scale of the axes to get the required data points and do a linear fit over these data points. After doing a linear fit based on the trendline, an equation of line is computed. For each equation of the linear fits (under both light and dark conditions) one must do manual calculations using the slope and intercepts to get the required diode parameters (including the value of kT : product of Boltzmann constant and temperature). This is time consuming and increases risk of mistakes while doing calculations. Also, it is tedious and a laborious task for a person while altering the linear fits on the analyzed data to obtain the desired correlation and recalculate the slope and intercepts. Excel can be considered as an obsolete tool for diode analysis. Origin has more advantages compared to Excel. Using Origin, it is easier for the user to alter the axes scale and observe the plots. The plots of the analysis appear to be more explicit and clearer. Doing a linear fit on the main data is also more convenient than in Excel, and it is less error prone as well. However, Origin has some limitations too. It is not a user-friendly tool and performing the analysis using Origin is also laborious and time-consuming. It becomes a lengthy and monotonous job when analyzing number of samples and storing the diode parameters results. The parameters from one step of the analysis are needed in the next step hence making the whole process of diode analysis complicated while using Excel or Origin. DioMac can overcome the issues where Excel and Origin fail. In DioMac one can feed in a text-file containing the measured J-V data of a sample and analyze the cell under light and dark conditions, perform linear fit on the data and accordingly obtain the diode parameters from the equation of the linear fits without doing manual steps in the calculations. DioMac provides a user-intuitive interface where the user can analyze numerous samples quickly without causing inconvenience in the usage and generate

accurate results consuming less amount of time. DioMac is a powerful tool which will alleviate all kinds of limitations, difficulties which one faces when using Excel or Origin. It also helps the users to do a thorough study of the behavior of the solar cell samples. This program will also take pictures in .png format of the final analysis plots and store them in a folder.

3.4 DioMac Program and its Features.

DioMac stands for Diode Analysis Machine. The main front panel window of the program is as shown in Figure 3.3.

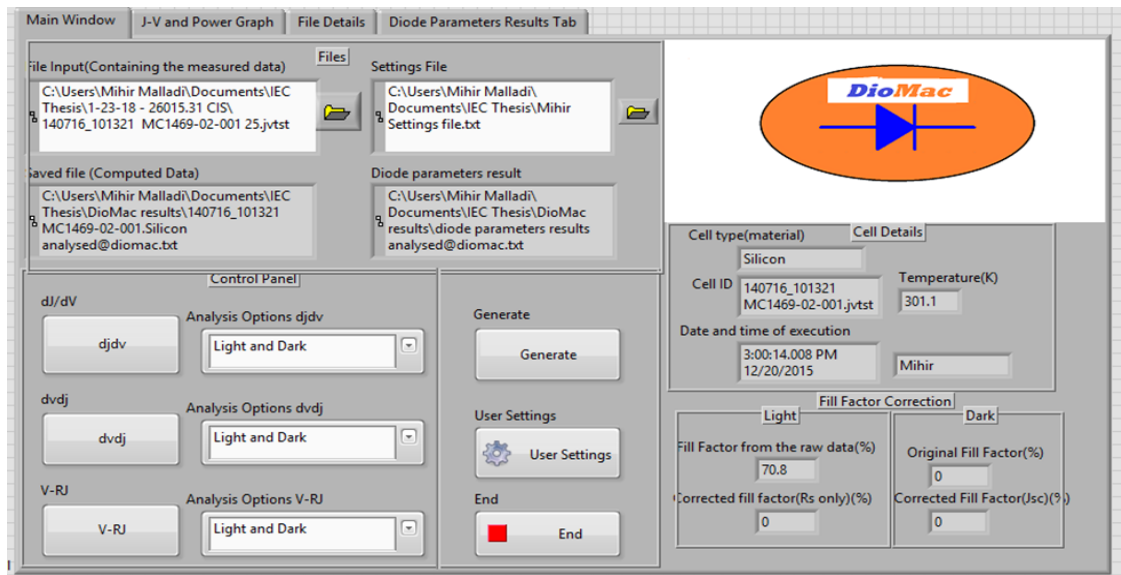


Figure 3.3. The front panel main menu window of DioMac. Comprises of four tabs: Main Window, J-V and Power Graph, File Details, Diode Parameters Results Tab.

I have designed a logo for DioMac as shown in Figure 3.4. The diode symbol represents the diode nature of solar cell with an orange background representing the color of the sun.



Figure 3.4 Logo of DioMac program.

The Main Window is as shown in Figure 3.3. There are four panels indicated by four tabs. In the first unit of the main panel there is a provision for uploading the input text file of the measured J-V data and user settings file for adjusting in the program according to the user's convenience. The second unit is the control unit which comprises of a menu for performing the diode analysis and tabulating the diode parameters results. The third unit comprises of the details related to the file such as cell type (type of solar cell), cell ID (used for identifying a solar cell sample), temperature, date and time of when a sample has been analyzed, and the user-name. The second panel in the next tab comprises of the J-V curve plots and associated power graph. The third panel reflects the data copied by the program from the loaded text file. From this panel the program uses the data relevant to carry out diode

analysis. The fourth panel consists of a table that records the end diode parameter results and copies the same to a text file generated by DioMac.

3.5 Development of the Program and its Working

The main basis on which this program operates is a state machine. A state machine is an architecture frequently used by LabVIEW programmers to develop applications [14]. A finite state machine is a model used in computation theory, for developing applications/programs that are meant to operate automatically or semi-automatically with less human interference. This is also called finite automation. Some real-life examples are automatic door systems, found at supermarkets and shopping malls [15], turnstile gates found at subway stations, and bus stations, and vending machines [14]. In LabVIEW a state-machine can be easily made using while-loops, case structures, and ‘enum’ operators. An enum stands for enumerator data type in computer programming. In LabVIEW enum constant is used to declare the names of the states that are part of a state machine. Based on the state-machine architecture, the flow diagram of DioMac is given in Figure 3.6 describing its mechanism. With reference to this flow diagram the program comprises of five states: J-V curve plotting, Wait for an Event state, djdv state, dvdj state, V-RJ state, End of Analysis state. Each of these states are described below:

- 1) **J-V Curve Plotting**: This state is automatically activated as soon as the program takes in the data from the input text file created by the J-V tester equipment at IEC. This state consists of a sub VI (equivalent to a subroutine or an invoked function) that plots the J-V curve under the light and dark conditions extracting the measured values from the file (in Figure 3.5).

Once the J-V curve and power graph have been plotted, the control is shifted to “wait for an event” state.

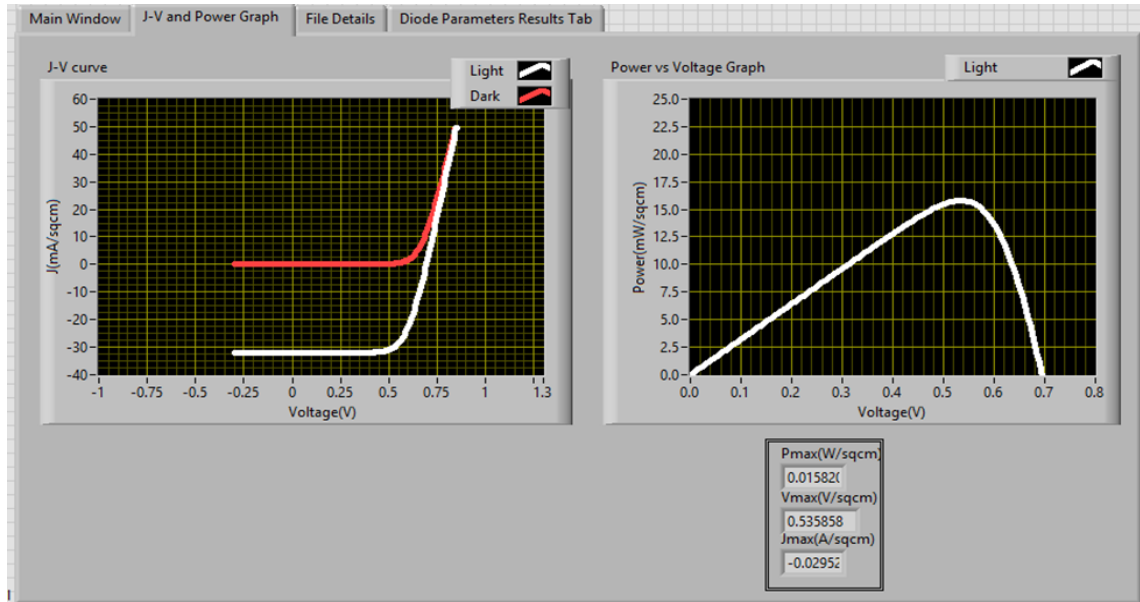


Figure 3.5 The J-V curve under both Light and Dark conditions (to the left) and the power graph of J-V in light (to the right)

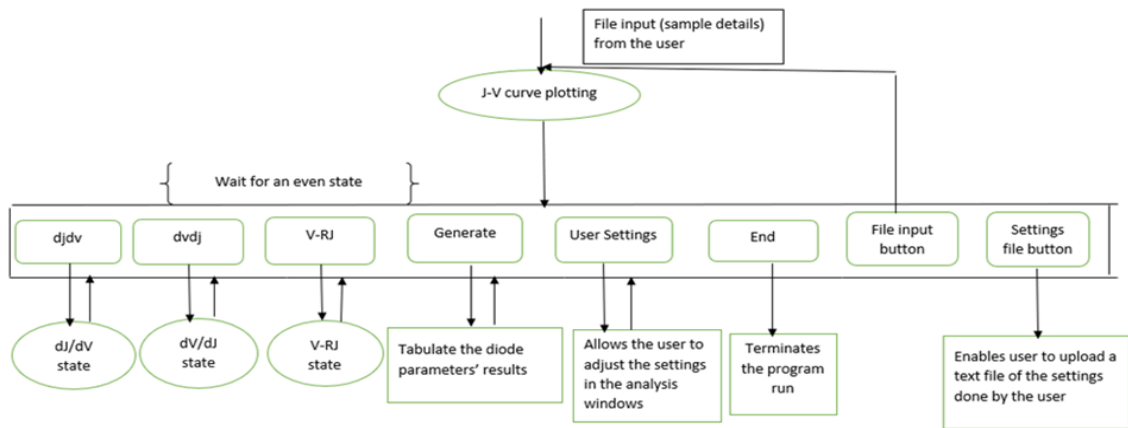


Figure 3.6 The flow diagram of DioMac depicting the working and flow of control.

2) **Wait for an Event State:** This state gives the user the discretion to choose the buttons in the control panel of the main window (referring to Figure 3.3). The control panel comprises of the following buttons:

- (i) **‘djdv’ Button:** This button will direct the user to the **djdv state** to perform the second part of the diode analysis. Once completed the control comes back to the **Wait for an Event** state.
- (ii) **‘dvdj’ Button:** This button will direct the user to the **dvdj state** to perform the third part of the diode analysis. Once completed the control comes back to the **Wait for an Event** state.
- (iii) **‘V-RJ’ Button:** This button will direct the user to the **V-RJ state** to perform the fourth part of the diode analysis. Once completed the control comes back to the **Wait for an Event** state.
- (iv) **‘Generate’ Button:** This button will enable the user to record and tabulate the diode parameter results of a sample’s data under execution. The tabulated data will be stored in a text file. **‘Generate’** button will also enable the program to create a text file containing all the calculations.
- (v) **‘User Settings’ Button:** This button allows the user to do adjustments for changing the range of the axis scales and adjusting the sliders for the linear fits according to his/her convenience.

- (vi) **‘End’ Button:** This button will take the control of the program to **‘End of Analysis’** state which will terminate the execution of the program.
 - (vii) **File Input and Settings Buttons:** These buttons are present in the File section on the main window. These buttons are LabVIEW’s file path controls. By clicking on the file input button, the user can upload another sample’s J-V file into the program to start afresh new analysis. The flow of control starts from the first state as shown in Figure 3.6. The settings file is used for uploading an existing text file containing the values for adjusting the sliders and axes scales.
- 3) **djdv State:** This state assists the user to perform the second part of diode analysis helping the user to extract the parameters G_{sh} (shunt) from the intercept of the linear fit over the range of data dJ/dV vs Voltage in reverse biased region. Once this state has been activated, the user can select the type of condition (viz. Light, Dark, Light and Dark) under which the respective data needs to be analyzed from the associated drop-down menu. Once the user selects the option the associated front panel appears allowing the user to observe the data and perform the second part of the diode analysis. The results obtained from the ‘Light and Dark’ option only will be recorded. The other conditions - ‘Light’ and ‘Dark’ separately - are meant for the user only to observe the data and linear fits but not for recording and storing the obtained parameters. The front panel of the ‘Light and Dark’ option is shown in Figure 3.7. The ‘scale settings’ button is for adjusting the range of axes’ sliders which

are used for adjusting the scale of the axes. Linear fitting toolbox consists of the sliders needed for fitting the data on the light and dark plots. The ‘Done’ button is for terminating the analysis window. After the button has been pressed a snapshot of the graph is taken and stored in a folder.

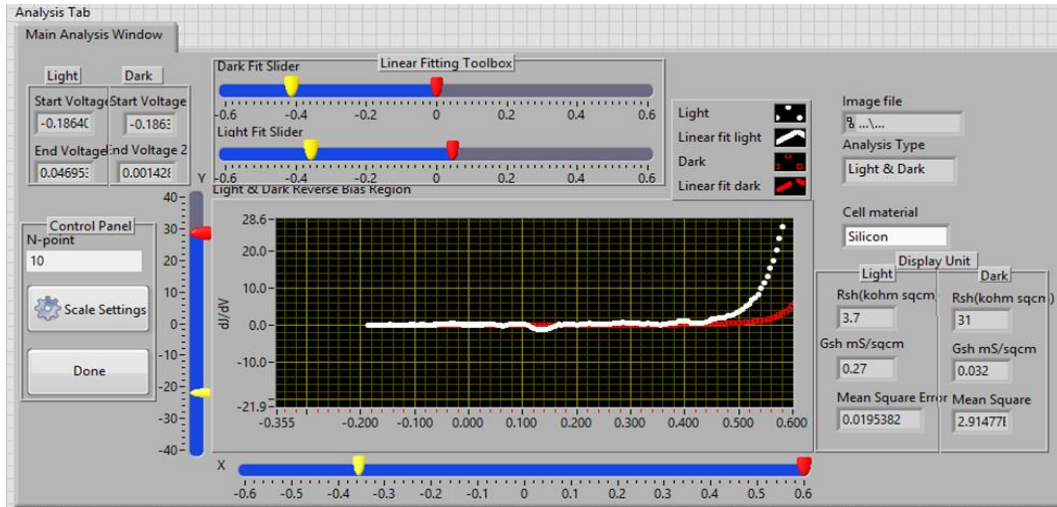


Figure 3.7 The front panel view of the second part of diode analysis under ‘**Light and Dark**’ conditions. Light data is in white color and the red is for Dark data.

- 4) **dvdj State:** This state assists the user to perform the third part of diode analysis for obtaining the parameters R_s (series resistance) and ideality factor (A) from the slope and intercept of a straight line respectively fitted over the data dV/dJ and $(J+J_{sc})^{-1}$. Once this state has been activated, the user can select the type of condition (viz. Light, Dark, Light and Dark) under which the respective data needs to be analyzed from the associated drop-down menu. Once the user selects the option the associated front panel appears allowing the user to observe the data and perform the third part of the diode analysis. The

results obtained from the 'Light and Dark' option only will be recorded. The other conditions 'Light' and 'Dark' options are meant for the user only to observe the data and linear fits but not for recording and storing the obtained parameters. The front panel view of the 'Light and Dark' conditions of the third part is shown in Figure 3.8. The 'scale settings' button is for adjusting the range of axes' sliders which are used for adjusting the scale of the axes. Linear fitting toolbox consists of the sliders needed for fitting the data on the light and dark plots. The 'Extend' buttons in the linear fitting toolbox are used for extending the linear fits. The 'Done' button is for terminating the analysis window. After the button has been pressed the parameters are recorded and snapshot of the graph is taken and stored in a folder.

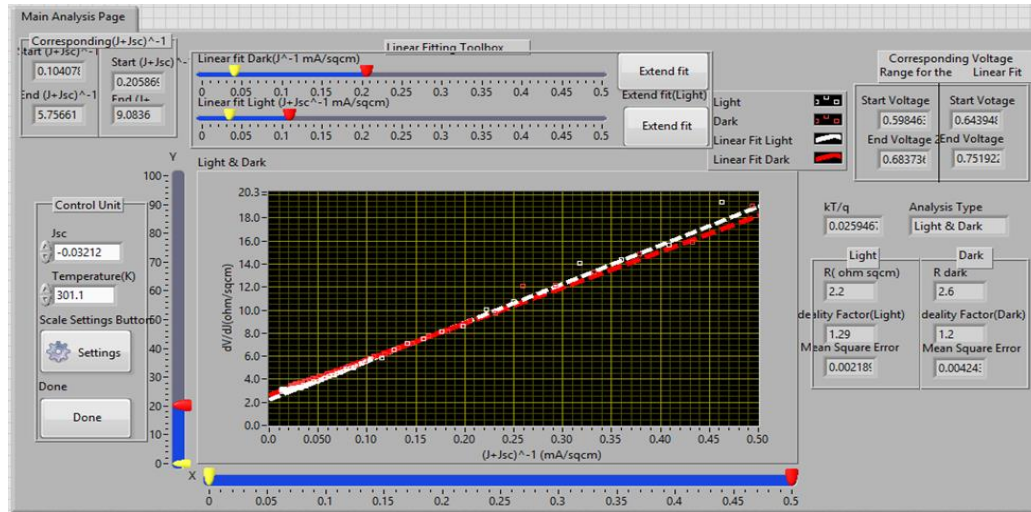


Figure 3.8 The front panel view of the third part of diode analysis under ‘**Light and Dark**’ conditions. Light data is in white color and the red is for Dark data.

- 5) **V-RJ State:** This state helps the user to perform the last part of the diode analysis to obtain the current J_0 and ideality factor from the intercept and the slope of straight line fitted over the logarithmic $\ln(J+J_{sc}-GV)$ and V-RJ data. This state acquires and utilizes the values of R_s , G_{sh} required for performing the calculations relevant to the fourth part. Once this state has been activated, the user can select the type of condition (viz. Light, Dark, Light and Dark) under which the respective data needs to be analyzed from the associated drop-down menu. Once the user selects the option the associated front panel appears allowing the user to observe the data and perform the fourth part of the diode analysis. The results obtained from the ‘Light and Dark’ option only will be recorded. The other conditions ‘Light’ and ‘Dark’ options are meant for the user only to observe the data and linear fits but not for recording and storing the obtained parameters. The front panel view of the ‘Light and Dark’

conditions of the fourth part is shown in Figure 3.9. The 'scale settings' button is for adjusting the range of axes' sliders which are used for adjusting the scale of the axes. Linear fitting toolbox consists of the sliders needed for fitting the data on the light and dark plots. The 'Extend' buttons in the linear fitting toolbox are used for extending the linear fits. The 'Done' button is for terminating the analysis window. After the button has been pressed a snapshot of the graph and the voltage correction plots (including the associated power graphs) is taken and stored in a folder. Figure 3.10. consists of the plots for correction in the J-V graph due series, and series and shunt resistances (in Light) and influence of J_{sc} on the Dark J-V curve. Power graphs of these voltage corrections are also shown in Figure 3.10. In the front panel of this analysis 'Manipulate' button is meant for the user to enter values for the series resistance and shunt conductance to observe the behavior of the semi-logarithmic plot. Once observed 'Proceed' button can be pressed to retain these values obtained from the previous parts of the analysis.

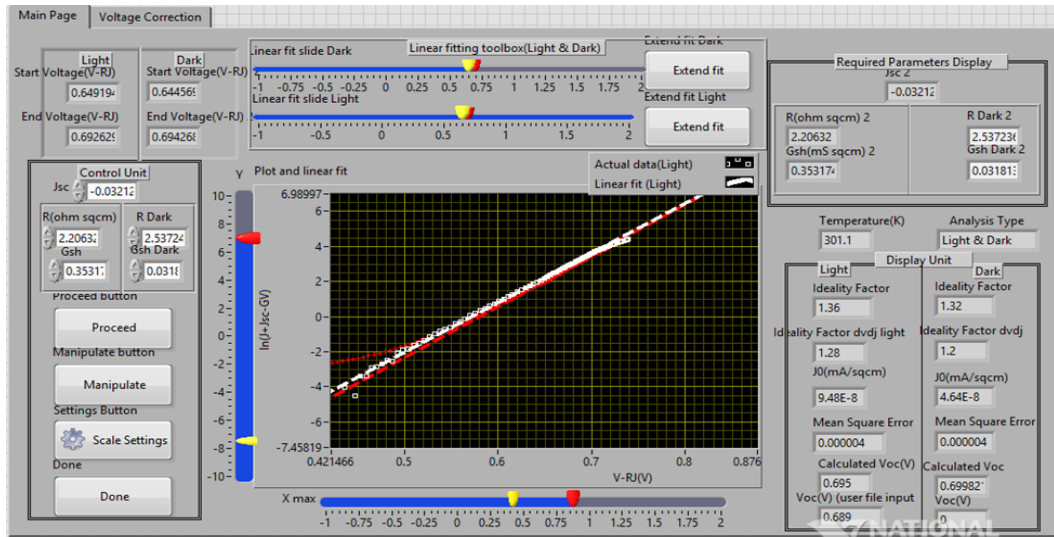


Figure 3.9. Front panel view of the fourth part of the diode analysis. White plot is for the Light data and red plot is for the dark data.

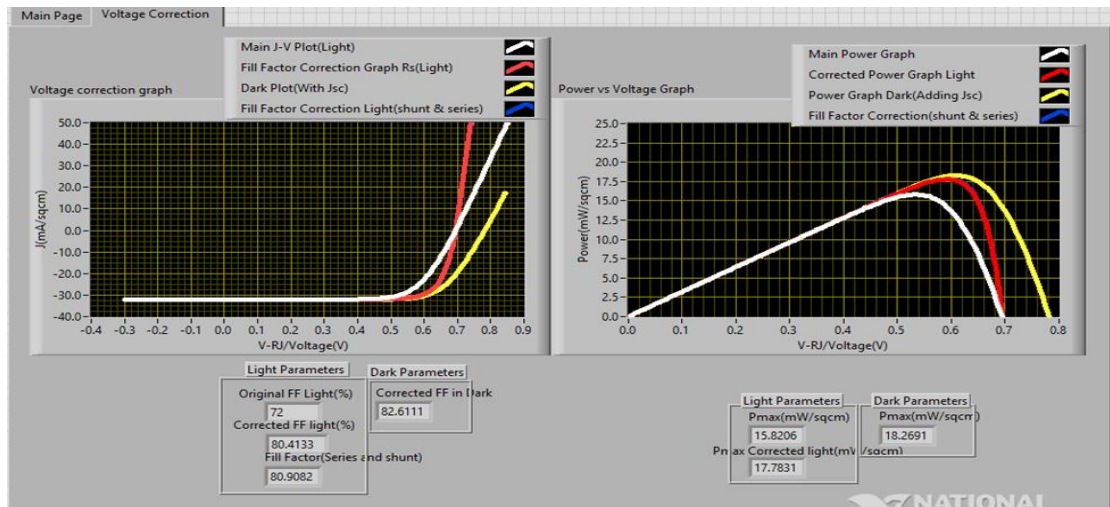


Figure 3.10 Voltage correction plots for the light and dark data. White plot is for the original J-V curve, color red represents correction due to series resistance, blue for correction due to series and resistances, and yellow is for the dark data (due to J_{sc}).

- 6) **'End of Analysis' State:** This is the final state of DioMac's state machine architecture. This state is activated by the 'End' button. This state will terminate the execution of the program.

APPLICATION OF THE PROGRAM ON Cu(In,Ga)Se₂ SOLAR CELL SAMPLES

4.1 Overview of the chapter

This chapter will talk about the application of the DioMac program in calculating the diode parameters based on its current-voltage characteristics at various temperatures for CIGS/CIS solar cell samples measured at IEC. In this chapter the following will be covered:

- 1) Analysis of CuInSe₂ solar cell sample and its behavior at different temperatures based on the J-V data measured under these temperature conditions.
- 2) Analysis of Cu(In,Ga)Se₂ solar cell samples prepared with CIGS baseline runs. One sample has high fill factor, and another with a low fill factor.
- 3) Analysis of a CIGS solar cell sample which shows anomalous behavior in the current-voltage characteristics.

4.2 Cu(In,Ga) Se₂ solar cells

Cu(In,Ga)Se₂ or CIGS solar cells are thin-film solar cells(TFSC) which are considered as one of the most promising cost -effective power generating solar cells [16]. These solar cells comprise of the CIGS compound which is a p-type semiconducting material(or the absorber layer). The CdS deposited acts as an n-type semiconductor(buffer layer). A p-n junction is formed between by CIGS and CdS.

CIGS is a I-III-VI semiconductor alloy that has two endpoints: CuInSe_2 and CuGaSe_2 [2]. These materials have chalcopyrite crystal structure. Alloying CuInSe_2 with CuGaSe_2 increases the bandgap. The schematic of a CIGS solar cell is given in Figure 4.1. Molybdenum is the metal contact used in CIGS cells. Substrate is soda lime glass substrates. Thompson in [2] gives a detailed description about the layers in the CIGS structure, and preparation of the solar cells. In [2] the measurement technique used for obtaining the current-voltage data, and understanding the optical losses using quantum efficiency has also been explained in detail. A more in-depth explanation of the methods and processes involved for preparation of these samples and the techniques used to provide a thorough study of these cells is given in [16] by William Shafarman.

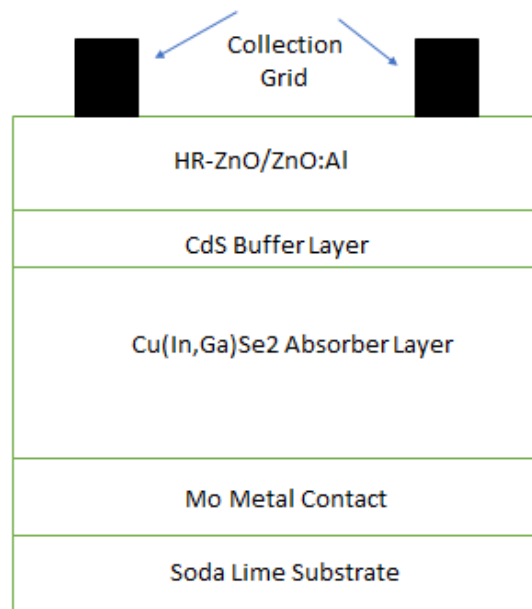


Figure 4.1. Schematic of a CIGS solar cell.

4.3 Applying DioMac on CuInSe₂ Sample at Different Temperatures

In this section I shall discuss how DioMac can be used in analyzing the CIS (CuInSe₂) solar cell at different temperatures. The sample under study was fabricated by fellow graduate student Nicholas Valdes at IEC and measured under different temperatures. The sample was fabricated in a method similar to one mentioned in the paper [17]. The analysis done by the program on this CIS sample is divided into four cases. In each of these cases an analytical model has been constructed by substituting the obtained diode parameters in the diode equation. The R² values (re-scaled mean squared errors) in Table 4.1 have been calculated from the analytical model data and the measured current-voltage data. These R² values can help in finding out if the analytical model fits well with the measured J-V data.

Case(i): Analysis and observation of the sample at room temperature (25-degree Celsius)

At the room temperature the solar cell behaves well and the diode model in [7] can be applied easily under this condition. Figure 4.2. shows the behavior of the sample under room temperature based on the measured J-V data at this temperature. There are no barriers and the ideality factors under both light and dark conditions range between 1 and 2. An analytical model of the J-V curve is has been plotted by substituting the values of diode parameters obtained into the diode equation in excel and compared with the measured J-V curve. Figure 4.3 shows these plots comparing the analytical J-V curve with that of the measured J-V data. From these plots we can conclude that the sample under the room temperature behaves well like a p-n junction diode.

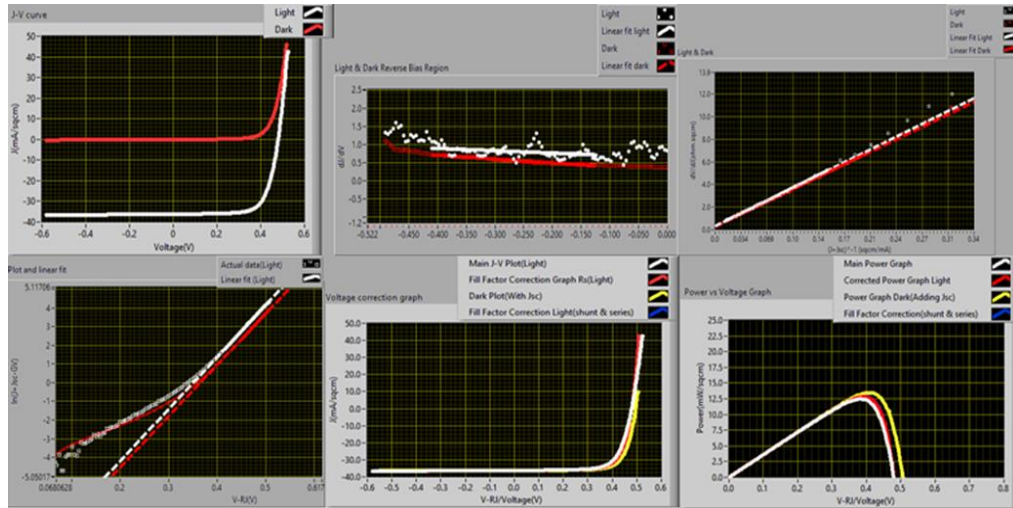


Figure 4.2. Analysis plots of the CIS solar cell sample at room temperature. a) The J-V curve b) dJ/dV vs Voltage c) dV/dJ vs $(J+J_{sc})^{-1}$ d) $\ln(J+J_{sc}-GV)$ vs $V-RJ$ e) J-V correction due to parasitic losses in light and dark f) Power vs Voltage graphs associated with the results in e)

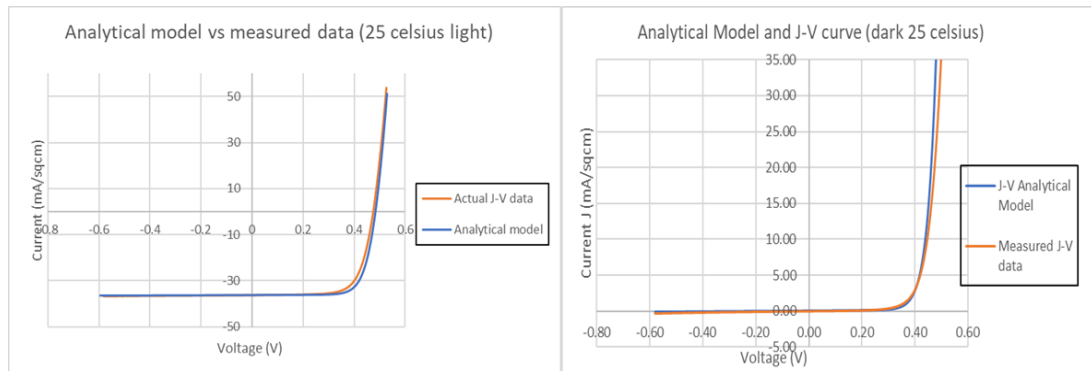


Figure 4.3 Plots showing the comparison between the analytical model and measured data in light and dark at 25 Celsius.

Case(ii) Analysis and observation of the sample at 45-degree celsius

The device behaves like the condition mentioned in case (i). The diode model is applicable under 45 degree Celsius also. The ideality factor is between 1 and 2 ranges. Figure 4.5 shows the plots for the analytical models made in light and dark from the obtained diode parameters and compared with the measured current-voltage data . The R^2 value between the analytical curve and the measured curve is shown in Table 4.1. From these plots we can say that the sample under this temperature behaves like a diode under both light and dark similar to the previous case. Hence the solar cell behaves well in this temperature.

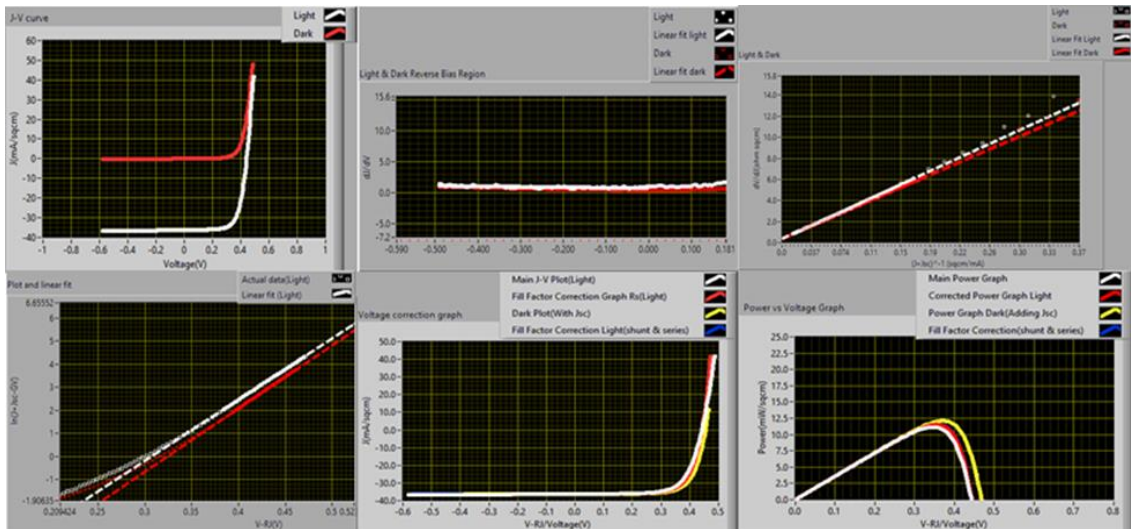


Figure 4.4 Analysis plots of the CIS solar cell sample at 45 Celsius temperature. a) The J-V curve b) dJ/dV vs Voltage c) dV/dJ vs $(J+J_{sc})^{-1}$ d) $\ln(J+J_{sc}-GV)$ vs $V-RJ$ e) J-V correction due to parasitic losses in light and dark f) Power vs Voltage graphs associated with the results in e)

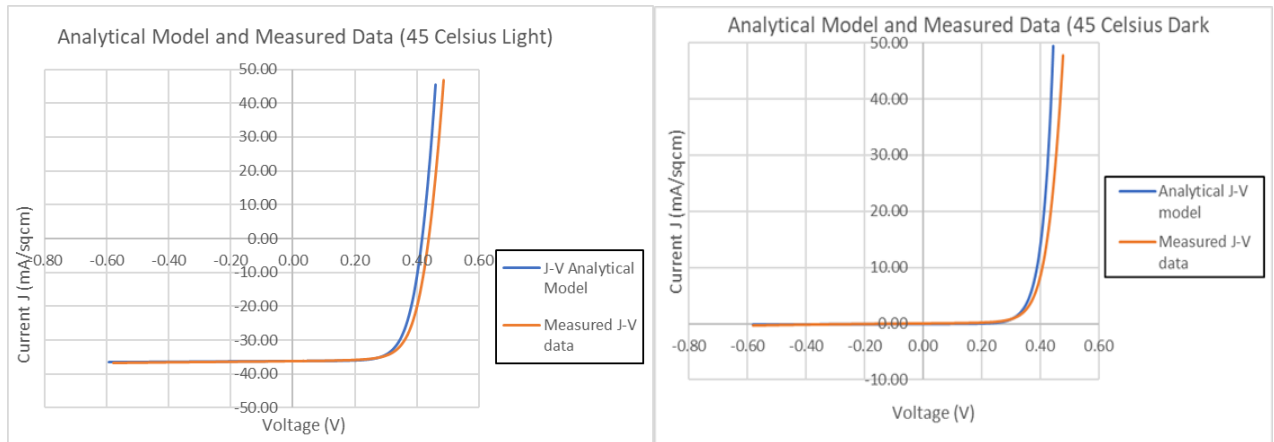


Figure 4.5 Plots of the analytical model and measured J-V data for the solar cell in light and dark under 45 Celsius temperature.

Case(iii) Analysis and observation of the sample at -55-degree Celsius

In this case the light J-V curve appears to be normal while the dark J-V curve is showing a tendency of blocking behavior in the forward biased region. In part 3 of the analysis in dark (dV/dJ vs $1/J$) there is a slight barrier towards the origin of the graph showing the nature of blocking behavior. In this part of the analysis for the dark curve a linear fit has been done in the region above the barrier. The plot between the analytical model and J-V measured data is shown Figure. 4.7. There is a difference in the curves in the light condition however the model fits well in the dark with R^2 correlation of 0.99. The diode model fits well on the dark data from the plot in Figure 4.7.

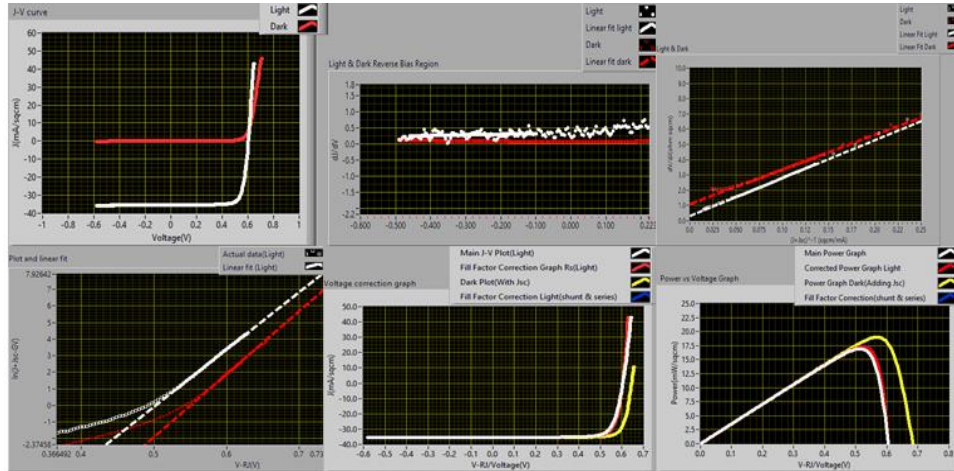


Figure 4.6 Analysis plots of the CIS solar cell sample at -55 Celsius. a) The J-V curve b) dJ/dV vs Voltage c) dV/dJ vs $(J+J_{sc})^{-1}$ d) $\ln(J+J_{sc}-GV)$ vs $V-RJ$ e) J-V correction due to parasitic losses in light and dark f) Power vs Voltage graphs associated with the results in e)

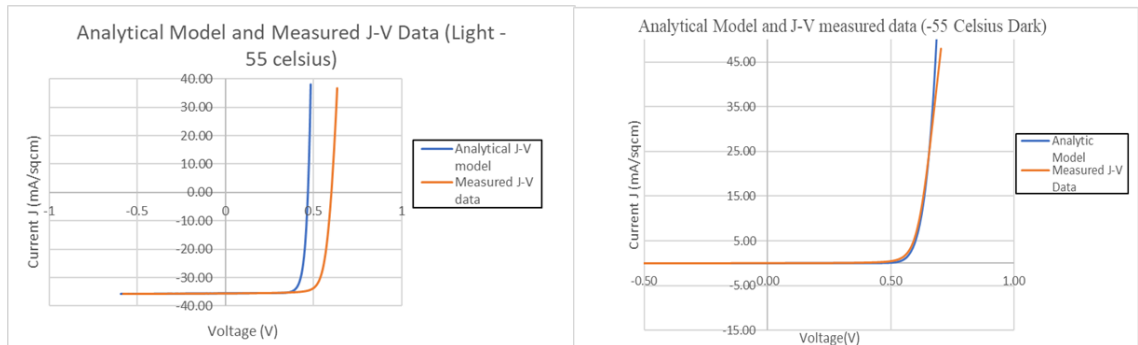


Figure 4.7 The analytical model and the measured J-V data for the sample at temperature -55 Celsius.

Case(iv) Analysis and observation of the sample at -75-degree Celsius

In this case there is a difference in the dark J-V curve compared to the previous case (i.e -55 Celsius). There is an increase in the barrier height for the dark data in the dV/dJ vs $1/(J+J_{sc})$ plot as shown in Figure 4.8. The dark data shows blocking behavior as explained in [7]. A linear fit above the barrier region will give the ideality factor between 1 and 2. From the plots in Figure 4.9 the analytical model fits well with the measured data in light but in dark there is a difference in the plots which could be due to blocking effect. The diode model is still applicable in this case.

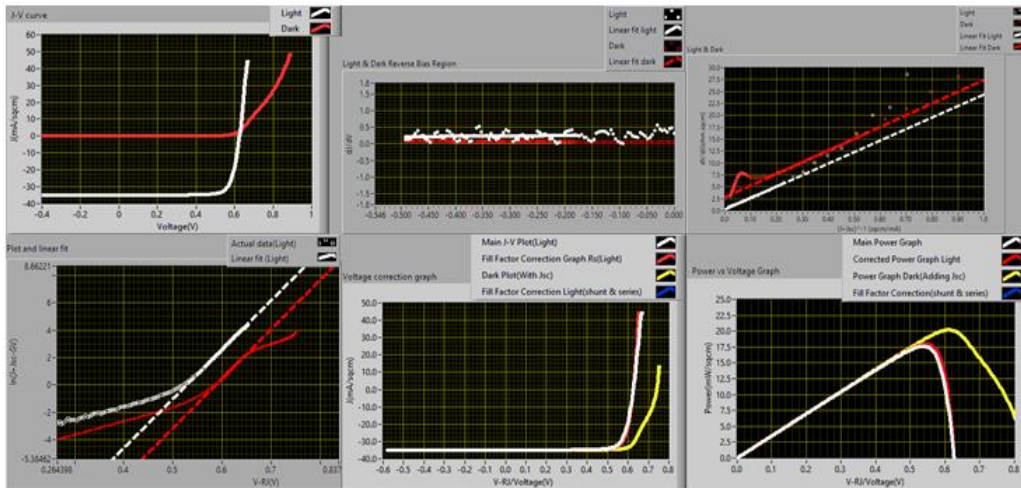


Figure 4.8 Analysis plots of the CIS solar cell sample at -75 Celsius. a) The J-V curve b) dJ/dV vs Voltage c) dV/dJ vs $(J+J_{sc})^{-1}$ d) $\ln(J+J_{sc}-GV)$ vs $V-RJ$ e) J-V correction due to parasitic losses in light and dark f) Power vs Voltage graphs associated with the results in e)

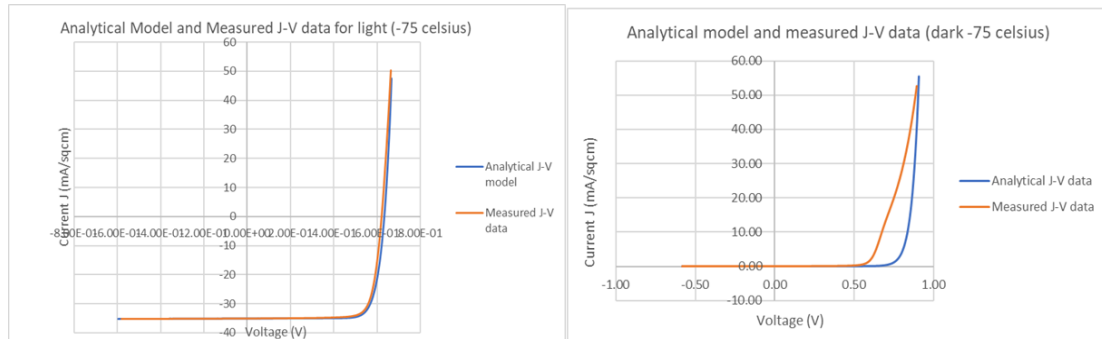


Figure 4.9 Analytical model and measured J-V data under light and dark conditions for the CIS sample at -75 Celsius.

Case(v)Analysis and observation of the sample at -105-degree Celsius

Under this condition the cell behaves badly in both Light and Dark condition. There has been a significant difference in the J-V curve in dark as shown in Figure. 4.10. In the part 3 of the diode analysis the plot in the Light condition has scattered data and is difficult to do a linear fit in the region to obtain series resistance and ideality factor. The diode model is not applicable in the dark data. The ideality factor obtained in the dark is 9.28 which does not go with the diode law. From Figure 4.11 the analytical model in dark does not fit well with the measured data hence the diode model is inapplicable to the dark J-V data at -105-degree Celsius temperature and the analysis cannot be done on the dark data.

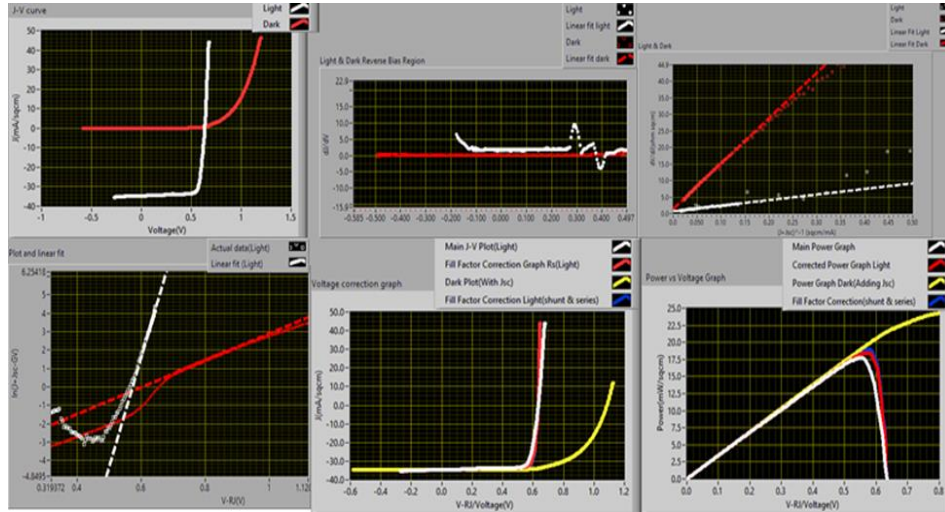


Figure 4.10 Analysis plots of the CIS solar cell sample at -105 Celsius. a) The J-V curve b) dJ/dV vs Voltage c) dV/dJ vs $(J+J_{sc})^{-1}$ d) $\ln(J+J_{sc}-GV)$ vs $V-RJ$ e) J-V correction due to parasitic losses in light and dark f) Power vs Voltage graphs associated with the results in e)

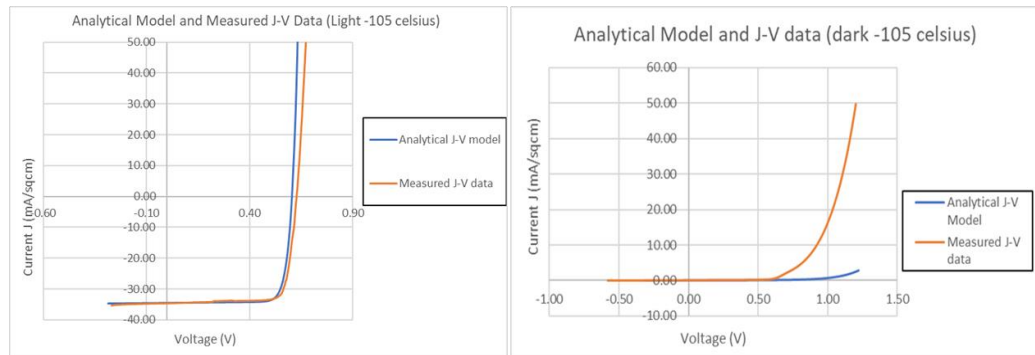


Figure 4.11 The J-V analytical model and the measured current voltage data for the CIS sample at -105 Celsius light and dark.

Table 4.1 The Table containing the R2 values between analytical model and measured data under light and dark for CIS sample at different temperatures

Temperature (Celsius)	Light (R2)	Dark (R2)
25	0.99	0.99
45	0.97	0.85
-55	0.78	0.99
-75	0.99	0.87
-105	0.85	0.79

Current-Voltage curves measured at low-temperatures show a blocking behavior due to a notch developed in the conduction band (that acts like a drain and traps electrons leading to recombination with the holes coming from the valence band of the band structure). Thus, a barrier is formed, and the electrons generated have insufficient energy to overcome this barrier [18]. Looking at the Table 4.1 the R² value of 0.85 can be the threshold to determine if analytical model of a J-V curve fits well with actual measured J-V data based on which we can infer that the diode parameters obtained from the analysis seem appropriate.

4.4 Application of Program on Cu(In,Ga)Se₂ Solar Cells with High and Low FF

The CIGS samples mentioned in this section were prepared by Dr. Kevin Dobson at IEC. These samples were prepared using baseline runs with CdS window layer. The sample named as sample A has a higher Fill Factor of 72% while the sample named as sample B has a higher Fill Factor of 65%. The measurements were taken at room temperature (25-degree Celsius). These cells have been analyzed by DioMac and the results are tabulated in Table 4.3.

The difference in the fill factors in these solar cell samples could be due to the photocurrent collection. The effect of $J_L(V)$ on the current-voltage characteristics

which has effect on the fill factor and V_{oc} [16]. From the Table 4.3 we can see that for Sample A the difference between the corrected fill factor in and the fill factor in dark due to J_{sc} is about 9%, while that of Sample B it is about 17%. The photo-collection difference can be due to the Ga concentration in these samples. The EDS and XRF data (characterization done in IEC by Kevin Dobson and Shannon Fields) as shown in Table 4.2. From this table Sample A has a lesser Ga/III. To further investigate the difference in the fill factor Quantum Efficiency (QE) technique is required. Other method that can be used to see if Ga gradient is a cause for reduction in the fill factor, is the depth profiling technique.

Table 4.2 EDS and XRF Data for the CIGS samples having high and low fill factors

Sample A (High FF)	EDS	(Cu)/(In+Ga)	0.79	Ga/(In+Ga)	0.30
	XRF	(Cu)/(In+Ga)	0.83	Ga/(In+Ga)	0.38
Sample B (Low FF)	EDS	(Cu)/(In+Ga)	0.79	Ga/(In+Ga)	0.41
	XRF	(Cu)/(In+Ga)	0.85	Ga/(In+Ga)	0.46

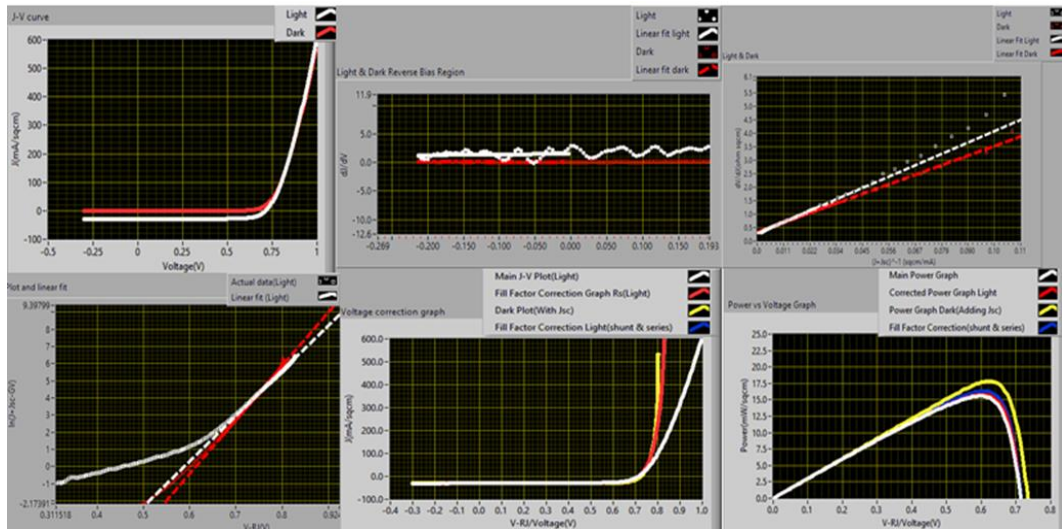


Figure 4.12 An example of CIGS solar cell with high Fill Factor prepared by Dr. Kevin Dobson. a) The J-V curve b) plot dJ/dV vs Voltage c) dV/dJ vs $(J+J_{sc})^{-1}$ d) $\ln(J+J_{sc}-GV)$ vs $V-RJ$ e) Voltage correction graphs in Light and Dark f) Power vs Voltage plot corresponding to plots in e)

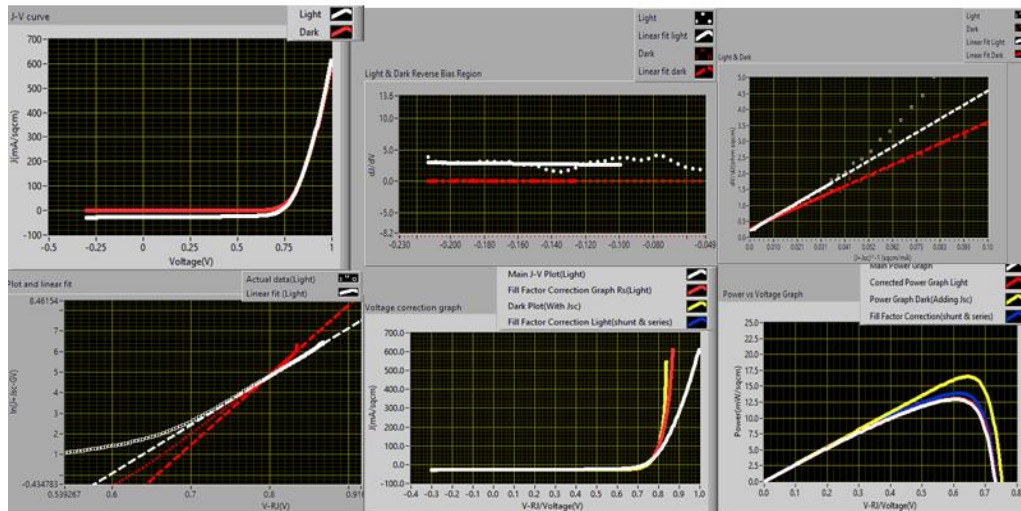


Figure 4.13 An example of CIGS solar cells with low Fill Factor prepared by Dr. Kevin Dobson. a) The J-V curve b) plot dJ/dV vs Voltage c) dV/dJ vs $(J+J_{sc})^{-1}$ d) $\ln(J+J_{sc}-GV)$ vs $V-RJ$ e) Correction of Voltages under Light and Dark due to parasitic losses. F) Corresponding Power vs Voltage plots

Table 4.3 Diode Parameters Results and Fill Factor correction under Light and Dark computed by DioMac for CIGS baseline run.

Sample	Voc (mV)	Jsc (mA/cm ²)	FF (%)	Gsh (mS/cm ²)	Rs (ohm-cm ²)	J0 (mA/cm ²)	A (dV/dJ)	A (V-RJ)	FF corrected (%)	Voc calculated (mV)
Sample A Light	709	30.4	71.8	2	0.3	1.30E-7	1.45	1.45	73.2	
Dark				0.073	0.3	1.70E-9	1.24	1.20	82.8	722
Sample B Light	726	27.3	65	2	0.2	9.6E-7	1.65	1.67	66	
Dark				0.081	0.29	3.8E-10	1.25	1.17	83.4	743

4.5 Applying Program in Analysis of an Anomalous Behavior of CIGS Solar Cell

This CIGS sample is prepared by CIGS experts at IEC. The substrate used here is borosilicate glass (in general soda lime glass is used). The diode model cannot be applied to this behavior. In the light J-V curve the behavior in the reverse biased region could be due to the voltage dependent photocurrent collection as described in [19]. The dark J-V data is flat in the reverse biased region. Non-ideal behavior in the cell can be seen in parts 3 and 4 of the diode analysis as shown in Figure 4.14 with barrier and blocking effect under both light and dark conditions. The possible reasons for the poor performance of this solar cell could be due to substrate or processing conditions in fabricating the device. The indiffusion of sodium from the soda-lime glass substrate increases the device performance.

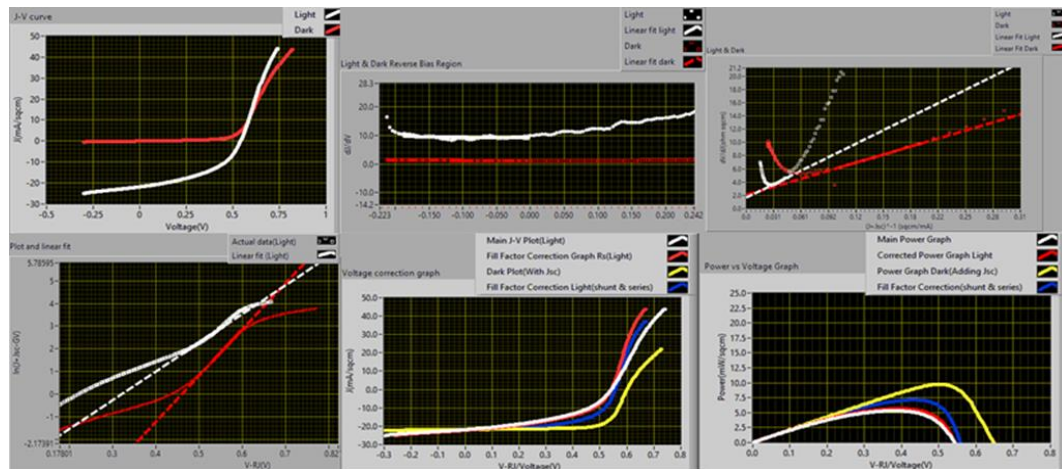


Figure 4.14 Example of a CIGS solar cell that does not follow the ideal diode model.
a) J-V curve b) dJ/dV vs Voltage c) dV/dJ vs $(J+J_{sc})^{-1}$ d) $\ln(J+J_{sc}-GV)$ vs V-RJ e) Voltage correction in light and dark f) power vs voltages

4.6 Conclusions

From the analysis of the CIS samples, and looking at the analytical models in light and dark and at the R^2 values in Table 4.1 it can be concluded that at higher temperatures (25 Celsius and 45 Celsius) the solar cell behaves well like a diode, but in lower temperatures (-55, -75, -105 Celsius) there is a degradation in the performance of the solar cell in the dark condition as the temperature decreases. The reason is that a barrier is formed at lower temperatures and the electrons have insufficient energy to overcome the barrier. For the CIGS solar cell samples with a low fill factor, some of the characterization techniques such as depth profiling and QE can be done to look at the Ga concentration profile which could be the main cause for the difference in the fill factors. The reason for the anomalous behavior of the CIGS solar cell in section 4.5 probably could be because of the substrate that is affecting the behavior. The program cannot be applied to this device since it does not follow the single diode model.

APPLICATION OF THE PROGRAM ON SILICON SOLAR CELL SAMPLES

5.1 Overview of the chapter

In this chapter the following solar cell samples' analysis will be discussed:

- 1) Analysis of Silicon FHJ and IBC solar cell samples made in the year 2014.
- 2) Analysis of Silicon solar cell samples prepared in the year 2018.
- 3) Comparing the 2014 cells' diode parameters to those of 2018 cells.
- 4) Analysis of Laser Fire Contact solar cells
- 5) Behavior of PEDOT:PSS solar cell samples used for degradation studies under Nitrogen.

In this chapter I shall show how DioMac can be applied to analyze Silicon based solar cell samples and help the user to observe and study the diode parameters.

5.2 Silicon Solar Cells Prepared in 2014.

These solar cell samples were prepared by an alumnus of IEC Judith Hsieh. The sample set comprises of two types of solar cells: Front Heterojunction (FHJ) and Interdigitated Back Contact (IBC). The structure and process of fabricating these solar cell samples are described in [20]. The cells are measured at room temperature 25 Celsius. The IBC solar cells have higher efficiency. The devices with Cell IDs MC 1497-09, MC 1503-04, MC 1483-06, MC 1483-10, MC 1492-02 are the IBC solar cells while the devices with

Cell IDs MC 1469-02, MC 1481-03, MC 1493-02 are FHJ solar cell devices

Table 5.1 Tabulated diode parameter results of IBC and FHJ Silicon solar cell samples analyzed by DioMac.

Sample	Voc (mV)	Jsc (mA/cm ²)	FF	Gsh (mS/sqcm)	Rs (ohm-cm ²)	J0 (mA/cm ²)	A (dV/dJ)	A (V-RJ)	Corr. FF	Voc Calc. (mV)
MC1503-04-IBC Light	621	32.7	72.2	0.18	0.6	4.7E-05	1.78	1.81	75.8	
				0.18	0.7	2.0E-06	1.38	1.48	79.6	749
Dark										
MC1483-10-IBC Light	653	38.6	72.7	0.40	0.7	1.1E-05	1.59	1.68	76.8	
				0.19	0.7	2.5E-06	1.44	1.55	79.8	633
Dark										
MC1483-06IBC- Light	589	38.4	71.0	0.83	0.7	3.5E-05	1.61	1.65	75.7	
				0.84	0.7	4.3E-06	1.32	1.46	79.7	665
Dark										
MC1497-09-IBC Light	588	29.3	72.7	0.78	0.7	1.2E-05	1.55	1.57	76.1	
				0.64	0.7	2.6E-06	1.33	1.44	79.0	605
Dark										
MC1492-02IBC- Light	677	37.8	72.8	0.22	0.5	9.5E-06	1.64	1.74	75.6	
				0.12	0.5	7.1E-07	1.40	1.51	80.7	602
Dark										
MC1469-02-FHJ Light	689	32.1	70.8	0.35	2.3	7.8E-08	1.23	1.35	80.7	
				0.03	2.6	2.8E-08	1.19	1.29	82.6	693
Dark										
MC1481-03-FHJ-Light	580	33.1	70.4	1.11	0.6	8.9E-06	1.40	1.50	73.9	
				0.49	0.6	2.2E-06	1.26	1.39	77.5	698
Dark										
MC1493-02-FHJ- Light	698	32.3	66.6	0.34	2.2	4.9E-06	1.71	1.73	75.8	
				0.002	2.3	3.6E-06	1.71	1.75	80.7	723
Dark										

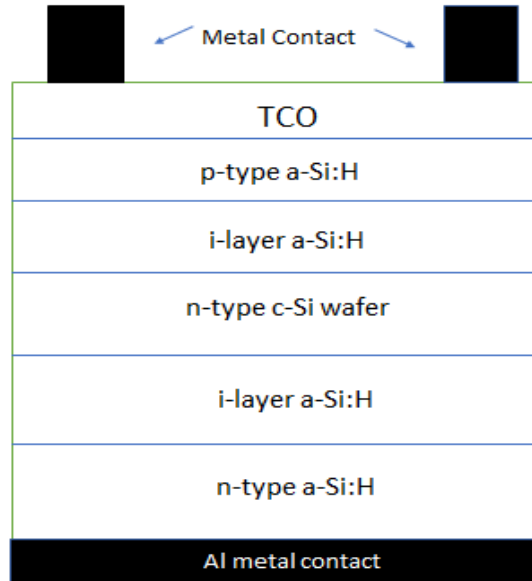


Figure 5.1 Schematic of a standard Silicon Front Heterojunction Solar Cell [20].

Table 5.1 shows the tabulated results of the diode parameters analyzed by DioMac for these samples.

5.3 Silicon Solar Cells Prepared in 2018.

These solar cells were prepared by an alumnus of IEC Ugochukwu Nsofor. These are front heterojunction silicon solar cells. Their efficiencies range from 18.4% to 20%. The devices are represented by the cell IDs MC 1650-01, MC 1642-09, MC 1652-02, MC 1657-20. The best of these samples has a high V_{oc} and higher Fill Factor. Table 5.2 shows the results of the diode parameters of these samples. The temperature is at 25 Celsius (room temperature).

Table 5.2 Tabulated results of solar cell samples made in the year 2018 analyzed by DioMac.

Sample	Voc (mV)	Jsc (mA/cm ²)	FF (%)	Gsh (mS/cm ²)	Rs (ohm cm ²)	J0 (mA/cm ²)	A dV/dJ	A V-RJ	Corr. FF (%)	Voc Calc. (mV)
MC1650-01 Light	696	35.68	74.0	0.2	1.0	9.4E-07	1.51	1.56	78.9	
Dark				0.003	1.0	6.6E-07	1.50	1.55	81.0	706
MC1642-09- Light	725	36.68	75.9	0.6	1.0	3.7E-08	1.34	1.37	80.9	
Dark				0.013	0.9	8.2E-08	1.33	1.45	82.6	711
MC1652-02- Light	717	34.89	75.8	0.2	1.2	2.0E-08	1.26	1.32	81.4	
Dark				0.1	1.2	1.2E-08	1.24	1.30	82.7	741
MC1657-20- Light	727	35.68	70.7	0.2	1.6	3.2E-06	1.69	1.76	77.8	
Dark				0.2	1.4	4.8E-06	1.75	1.86	81.0	727

5.4 Comparison of the diode parameter results for 2014 and 2018 samples

A comparison has been done between these IBC, FHJ solar cells made in 2014 with that of silicon solar cells made in the year 2018. The following parameters have been compared between these samples' data:

- 1) **Comparison based on the ideality factors under light and dark:** Here a comparison has been made for ideality factors under light and dark conditions. Two separate plots have been made representing the ideality factors calculated under part 3 of diode analysis (dv/dj vs $(J+J_{sc})^{-1}$) and those calculated under part 4 of the diode analysis (semilogarithmic plot of $J+J_{sc}$ vs $V-RJ$). The data from 2018 samples shows a linear behavior in both the plots as shown in Figure 5.2. In the case of 2014 samples there is no linear correlation between the light and dark ideality factors.

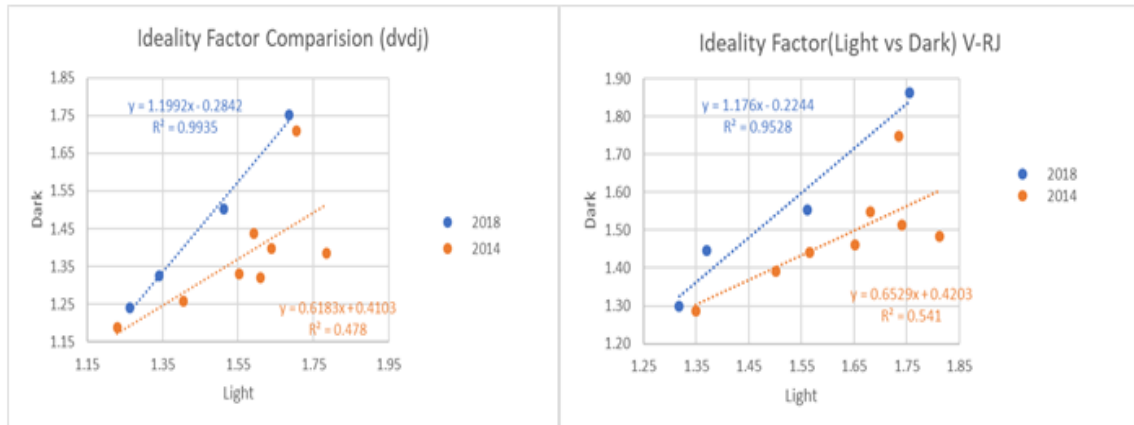


Figure 5.2 Plots representing the relationship between ideality factors under light and dark conditions. Plot (in left) are ideality factors calculated from part 3 and plot (in right) are ideality factors calculated from part 4 of diode analysis.

- 2) **Comparison of the series resistance (R_s) under Light and Dark:** The series resistance (R_s) obtained from the part 3 of the diode analysis (dV/dJ vs $(J+J_{sc})^{-1}$) under both light and dark conditions have been compared for both 2014 and 2018 samples. Their relationship under light and dark are shown in Figure 5.3. Both these sample sets show linear behavior with 2014 samples having a better correlation.

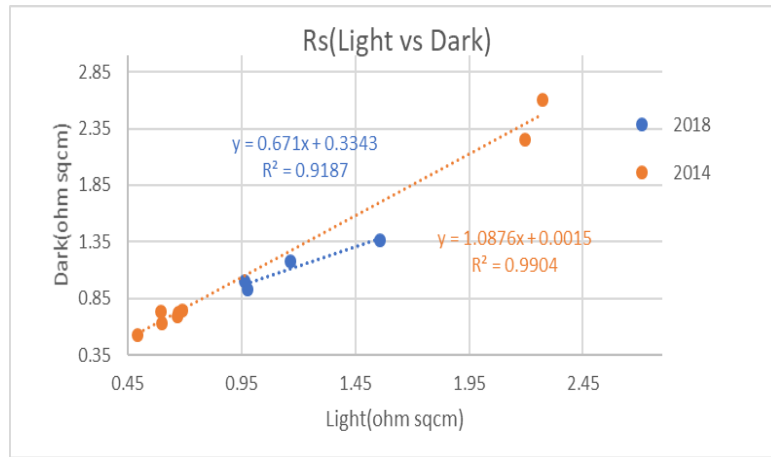


Figure 5.3 Plot showing the series resistance (light vs dark conditions) for 2014 and 2018 samples.

- 3) **Relation between V_{oc} and J_0 current:** Considering equations (2.6) and (2.7) from chapter 2 of this thesis we arrive at the linear relationship between $\ln(J_{sc}/J_0)$ and $V_{oc}q/nkT$. The parameter 'n' here is the ideality factor. The relationship between these two expressions is shown in Figure 5.4 under both light and dark conditions. The V_{oc} values in light have been measured under illumination while the V_{oc} values in the dark have been calculated using the ideality factor values obtained from part 4 of the analysis.

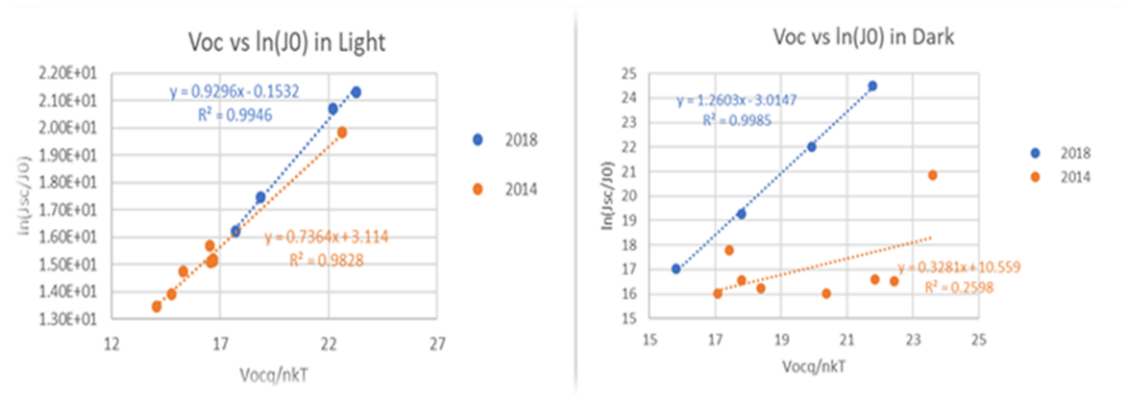


Figure 5.4 Plot of $V_{oc,q}/nkT$ vs $\ln(J_{sc}/J_0)$ under light and dark conditions respectively.

The 2018 samples show a linear behavior under both light and dark but in the case of the 2014 samples a linear relationship has been observed in light but there is no correlation in dark.

4) **Relation between Saturation Current Densities(J_0) under Light and Dark:**

Figure 5.5 shows the plot between J_0 calculated under Light and Dark using part 4 of the diode analysis. From the plot the samples of 2018 show a linear behavior but there is no correlation in the 2014 samples.

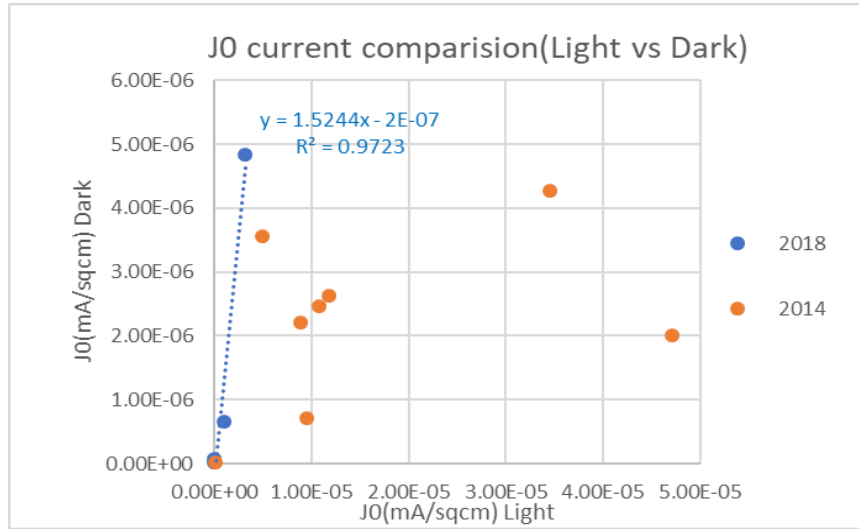


Figure 5.5 J₀ current comparison under Light and Dark for 2014 and 2018 samples

5) **Relationship between Fill Factor and Series Resistance (R_s):** To understand the relationship between the Fill Factor and the series resistance, a model has been proposed by Martin Green in [21]. The series resistance is considered as a parasitic loss that affects the fill factor. Here three type fill factors are calculated under light condition:- Using the original fill factor measured, corrected fill factor due to series resistance done by DioMac, and fill factor calculated based on the formula by Martin Green in [21]. In the dark the graphs are plotted between the corrected fill factor in dark, and fill factor calculated using the formula against the series resistance calculated. The formula of Martin Green is given by:

$$FF_s = FF_0(1 - r_s) \quad \text{-----(5.1)}$$

Where r_s is the characteristic series resistance which is given by $r_s = \frac{V_{oc}}{J_{sc}}$.

$$FF_0 = (v_{oc} - \ln(v_{oc} + 0.72)) / (v_{oc} + 1) \quad \text{-----(5.2)}$$

$$V_{oc} = \frac{V_{oc}}{V_{th}} \quad (V_{oc} = \text{normalized } V_{oc}, \text{ and } V_{th} = nkT/q) .$$

Figures 5.6 and 5.7 show the plots done under both Light and Dark conditions.

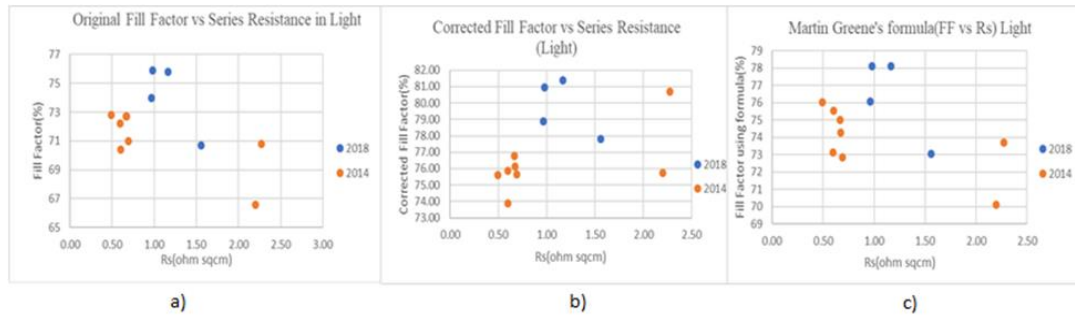


Figure 5.6 Plots for Fill Factors vs Series Resistance in light a) Graph using the original fill factors b) Using Corrected Fill Factors c) Using the formula

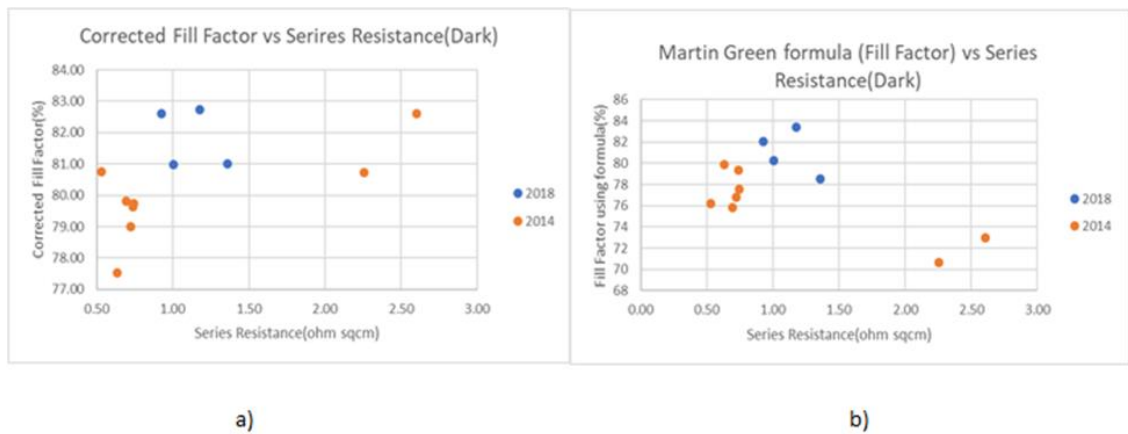


Figure 5.7 Plots for Fill Factors vs Series Resistance in dark a) Using Corrected Fill Factors b) Using the formula of Martin Green

From the plots in Figures 5.6 and 5.7 it is observed that for both the 2014 and 2018 samples sets there is no correlation between the fill factors calculated and the series resistances analyzed under both light and dark conditions of these cells.

6) **Relationship between Fill Factor and Ideality Factor:** To see if there is any relation between fill factor and ideality factor, the graphs have been plotted under light and dark. The fill factors values are same as the ones used in the comparison with series resistance. The plots in Figures 5.8 and 5.9 are for light and dark respectively.

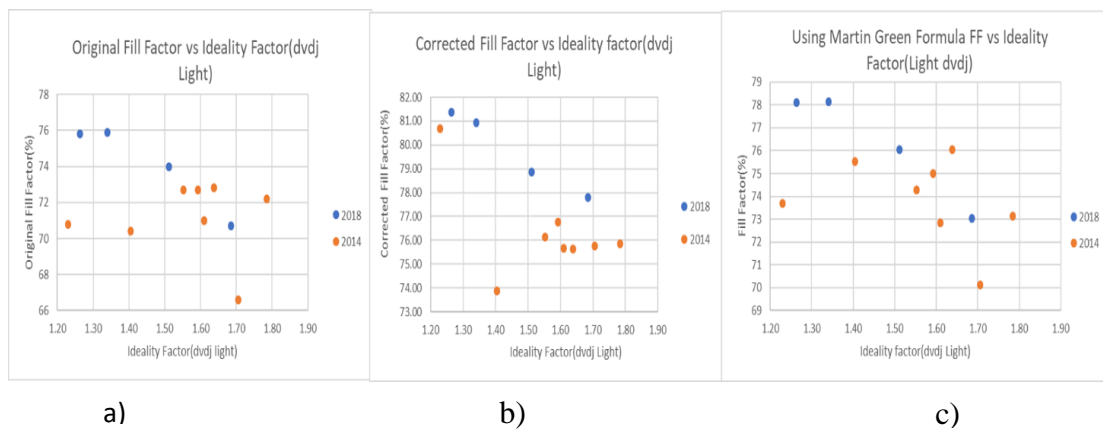


Figure 5.8 Plots for FF vs Ideality Factor a) Using Original Fill Factor b) Using Corrected Fill Factor c) Using the formula of Martin Green.

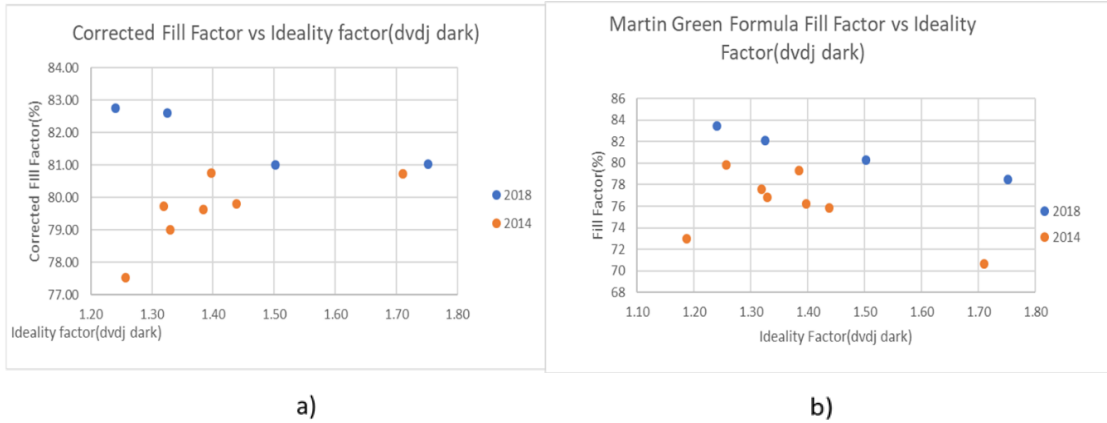


Figure 5.9 Plots for FF vs Ideality Factor in dark a) Corrected Fill Factor in dark b) Using Martin Green formula

From these plots we can see there that there is no linear relationship between ideality factors and the fill factors in all both in light and dark conditions. The ideality factor doesn't have an influence on the fill factor for these samples.

5.5 Laser Fire Contact Silicon Solar Cells

These solar cell samples have been prepared by using Laser-Fire Contact (LFC) also called as Laser Fire Spot (LFS). The description about Laser Fire Contact is mentioned in [22]. These silicon solar cell samples have been made by a PhD student from IEC, Nuha Ahmed. The samples with IDs MC 1690-04, and MC 1690-05 have been analyzed using DioMac program. Table 5.3 and 5.4 show the tabulated diode parameter results for MC 1690-04, and MC 1690-05 samples respectively

Table 5.3 Tabulated diode parameter results for the sample with cell ID MC 1690-04

Sample	Voc (mV)	Jsc (mA/cm ²)	FF (%)	Gsh (mS/cm ²)	Rs (ohm-cm ²)	J0 (mA/cm ²)	A (dV/dJ)	A (V-RJ)	Corr. FF (%)	Voc Calc. (mV)
pre-LFS Light	717	36.0	68.4	0.08	2.3	1.2E-06	1.56	1.63	78.5	
				0.006	2.4	1.3E-06	1.63	1.67	80.1	734
postLFS1 Light	709	36.7	67.3	0.82	2.1	9.1E-06	1.81	1.83	76.6	
				0.0003	2.0	3.1E-05	1.95	2.04	78.7	734
post-LFS2 Light	712	36.6	68	0.03	2.2	1.5E-06	1.60	1.64	78.1	
				0.006	2.2	5.9E-06	1.76	1.81	79.2	729
post-LFS3 Light	698	36.85	66.3	0.31	2.2	1.3E-06	1.55	1.59	76.4	
				0.004	2.2	1.0E-05	1.77	1.82	77.1	709

Table 5.4 Tabulated diode parameter results for the sample with cell ID MC 1690-05

Sample	Voc (mV)	Jsc (mA/cm ²)	FF (%)	Gsh (mS/cm ²)	Rs (ohm-cm2)	J0 (mA/cm ²)	A (dV/dJ)	A (V-RJ)	Corr. FF	Voc Calc. (mV)
pre-LFS Light	709	35.9	64.4	0.2	3.8	1.7E-09	1.14	1.16	81.4	
Dark				0.003	4.3	8.4E-07	1.63	1.60	81.5	724
postLFS1 Light	705	36.3	64.5	0.6	3.6	8.9E-09	1.18	1.24	80.9	
Dark				0.002	4.0	2.5E-06	1.73	1.71	81.1	724
post-LFS2 Light	701	36.0	63.2	1	3.7	5.7E-08	1.32	1.35	79.6	
Dark				0.002	4.1	9.3E-06	1.85	1.86	81.1	707

5.6 Hybrid Silicon Solar Cells using PEDOT: PSS Polymer

Hybrid silicon solar cells are prepared by depositing PEDOT:PSS (poly(3,4 ethylene dioxythiophene):poly (styrene sulfonate) on silicon using spin-coating technique. The PEDOT:PSS polymer behaves like a p-type contact over an n-type silicon. PEDOT:PSS can be used to make low-cost solar cells and it also enhances photo collection efficiency [23]. The sample has been prepared and measured by Abhishek Iyer, PhD student from the Department of Electrical and Computer Engineering who is using the solar cell to observe the degradation in the performance of the solar cells under Nitrogen storage. The performance of this sample has been observed for six weeks. The J-V measurements were taken for every week. The cell behaves badly and does not agree with the diode model as described in [7]. The solar cell does not have a single diode model. DioMac has analyzed the cell's data for each of the weeks and the part 3 of the diode analysis has been observed.

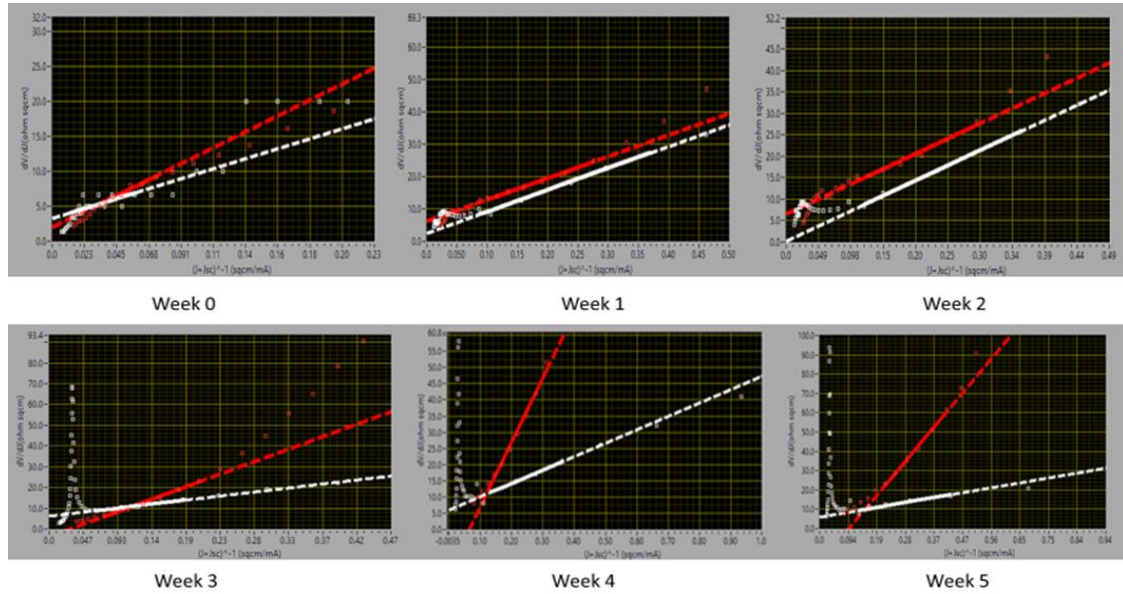


Figure 5.10 Plots of the 3rd part of diode analysis under light and dark for each week of observation

From Figure 5.10 we observe the light and dark plots for each of the six weeks starting from week 0 to week 5. In the dark the curve has been degrading and the linear fit cannot be done on these curves to obtain the series resistance. The ideality factors for these plots under dark are more than 2. In the light the barrier height has been increasing week by week. These plots show that diode analysis cannot be done on this solar cell sample.

CONCLUSIONS

In this work I discussed in brief about the importance of solar cells and then presented the standard equivalent circuit for a single diode model of a solar cell. In Chapter 1 and Chapter 2 the diode parameters and their importance in understanding the performance of solar cells was discussed. DioMac has been developed in LabVIEW to alleviate the issues generally faced when using Excel or Origin and provide a user-friendly interface making the user perform tasks at ease. It is a unique program created to analyze the measured current-voltage characteristics of solar cells of any material to extract more fundamental properties that would help the user to study and investigate the performance of these cells thoroughly. By partially automating some the analysis and graphing steps, DioMac will allow users to analyze numerous J-V data and generate the diode parameter results in less amount of time. The risk of committing errors while performing the diode analysis is also alleviated to a large extent by using the program. Another advantage of using DioMac is that the program will take the images of the plots of the four stages of diode analysis (inclusive of J-V correction curves under light and dark conditions and their associated power vs voltage plots.) in .png format and store them in the computer. The results of the diode parameter results will be tabulated and stored in a text file. The data calculated by the program under each of the four parts (i.e. computed data for current (J), voltage (V), dJ/dV , $(J+J_{sc})^{-1}$, dV/dJ , $\ln(J+J_{sc}-GV)$ and $V-RJ$) is also tabulated and recorded in text file containing the sample name and its filename. The other advantage of DioMac is

that once a sample's data has been analyzed and the results have been calculated, a new sample's J-V data can be loaded into the program and a fresh diode analysis can be performed. Hence one can perform the diode analysis on numerous samples' data and store results continuously without causing any kind of inconvenience or trouble in the usage. One can adjust the settings of the analysis tabs (such as the adjustments of the sliders that are used to observe the plots and perform linear fit on the data and adjust the value for numerical differentiation for part 2 of the analysis before opening the tab) according to his/her choice. The program provides a user-friendly interface allowing the user to analyze, observe and study the behavior of solar cell. This is useful to compare performance for example, under dark or illuminated conditions, as a function of temperature or as a function of storage time or subsequent annealing treatments. In the Chapters 4 and 5 the applications of this program on CIGS and Si solar cells has been discussed. From the results and the plots, we can infer that DioMac can be applied easily on the solar cells that follow single diode model based on the lumped circuit shown in Figure 1.2 under Chapter 1. However, the program cannot be used to on the solar cells that do not follow single diode model for example the anomalous behavior of a CIGS solar cell sample (in Chapter 4) and Hybrid Si solar cell sample using PEDOT:PSS polymer (in Chapter 5). This program can be opened in any of the latest LabVIEW versions and used by the scientist/researchers working on solar cells/photovoltaics.

REFERENCES

- [1] Reddy, P Jayarama., *Science and Technology of Photovoltaics*, BS Publications, 2nd Edition.
- [2] Thompson, C., *Thesis*, ‘Characterization of Photocurrent and Voltage Limitations of Cu(In,Ga)Se₂ Thin-Film Polycrystalline Solar Cells’, Department of Electrical and Computer Engineering, University of Delaware, Summer 2010
- [3] Steven Hegedus, Lecture Notes Class 5 and 6 Basic PV, Solar Energy Tech and Applications, Spring 2018.
- [4] Mertens, *Photovoltaics Fundamentals, Technology, and Practice*, Wiley, 2014
- [5] PV Education-<https://www.pveducation.org>.
- [6] Mudigonda, S, *Thesis*, ‘Characterization of fundamental parameters of front junction amorphous/crystalline silicon heterojunction solar cells using various electrical methods’, Dpeartment of Electrical and Computer Engineering, University of Delaware, Summer 2010.
- [7] S. S. Hegedus, W. N. Shafarman, “*Thin Film Solar Cells: Device Measurements and Analysis*”, *Prog. Photovolt: Res. Appl.* (2004) **12**: p 155-176.
- [8]. Böer, Karl, *Handbook of the Physics of Thin-Film Solar Cells*, Springer 2013.
- [9] Gray, Jeffery.L, *Handbook of Photovoltaic Science and Engineering*, Luque A., Hegedus S., Wiley, 2003, Chap.3. The Physics of Solar Cells
- [10] Ertugrul, N., *Towards Virtual Laboratories: a Survey of LabVIEW-based Teaching/Learning Tools and Future Trends*,*Int. J. Engng Ed. Vol 16. No.3 pp. 171-180, 2000.*
- [11] S. Sumathi, P.Surekha, *LabVIEW based Advanced Instrumentation Systems*, Springer.
- [12] LabVIEW Basics, Environment, National Instruments-<http://www.ni.com/getting-started/labview-basics/environment>

- [13] Benefits of Programming Graphically in NI LabVIEW, National Instruments-
www.ni.com/en-us/innovations/white-papers/13/benefits-of-programming-graphically-in-ni-labview.html
- [14] Tutorial: State Machines, National Instruments-
<http://www.ni.com/tutorial/7595/en/>
- [15] Michael Sipser, *Introduction to the Theory of Computation*, Thomson ,2nd edition.
- [16] Shafarman W.N., S. Siebentritt, L.Stolt, *Handbook of Photovoltaic Science and Engineering*, Luque A., Hegedus. S, Wiley, 2003. Chap. 13. Cu(In, Ga)Se₂ Solar Cells.
- [17] N.Valdes et al, “Ag Alloying and KF Treatment Effects on Low Bandgap CIGS Solar Cells”, *IEEE*, 45th PVSC 2018.
- [18] Adrian Chirilla et al. “Highly efficient Cu(In,Ga)Se₂ solar cells grown on flexible polymer films”, *Nature Materials*, Vol.10, November 2011.
- [19] S. Hegedus et al., *Voltage Dependent Photocurrent Collection on CdTe/CdS Solar Cells*, *Prog. Photovolt:Res.Appl.* 2007 ; 15:587-602.
- [20] Judith Hsieh, *Thesis*, ‘The Effect of Silicon and CIGS based Solar Cells Structure and Processing on Temperature Dependent Performance Losses’, Department of Electrical and Computer Engineering, University of Delaware, Fall 2014.
- [21] Martin. A. Green, *Solar Cell Fill Factors: General Graph and Empirical Expressions*, *Solid-State Electronics*, Vol 24, No.8, p.788-789, 1981.
- [22] U. Das et. al., *Effect of Dielectric layers on laser-fired-contact performance in a a-Si/c-Si heterojunction Solar Cells.*, 45th PVSC 2018.
- [23] A.Iyer et. al., *Effects of Co-Solvents on the Performance of PEDOT:PSS Films and Hybrid Photovoltaic Devices*, *Journal of Applied Sciences*, 2018.

Appendix A

FLOWCHART DIAGRAM FOR OBTAINING DERIVATIVES dJ/dV OR dV/dJ

A.1 Flowchart for numerical differentiation

Figure A.1 shows the flow chart diagram of the numerical differentiation used for computing dJ/dV data in part 2 of diode analysis and similar logic is used for obtaining dV/dJ in part 3 of the analysis . Once the user enters the analysis tab, he or she will be prompted to enter the number of points based on which the numerical differentiation will be performed. Referring to the flow chart, two arrays $J []$ and $V []$ containing the data of current and voltage respectively (extracted from the loaded text file). The user is then prompted to enter a value of N to perform an N -point numerical differentiation in computing dJ/dV meaning that N points is fit linearly, and the slope is used to define the derivative. The maximum number iterations in a loop is set by a variable `loop_count`. `DeleteFromArray ()` is a pseudo-code representing the **Delete from Array** icon in LabVIEW. This function is used to avoid repetition of previously used data points while computing data points from the current and voltage arrays. Pseudo-code `subset ()` from the flow chart represents the sub-array icon used in LabVIEW program that is meant to extract a sub array of current and voltage arrays using the limits as the loop counter ' i ' and variable N , extracting N set of data points (for eg. If $N=2$ then two data points set, and if $N= 10$ then ten data points set). On these N set of data points using **Linear Fit** function of current (Y-Variable) and voltage (X-variable). The resultant slope from this operation gives the array containing dJ/dV values. Plot between this dJ/dV array and the voltage (V) array we

get the main data of the second part of diode analysis. The same logic is applied for part 3 except that 2-point numerical differentiation is performed with the voltage array being the Y-variable and current array being the X-variable in order to compute dV/dJ array. Figure A.2 shows the snippet block diagram representation that performs dJ/dV .

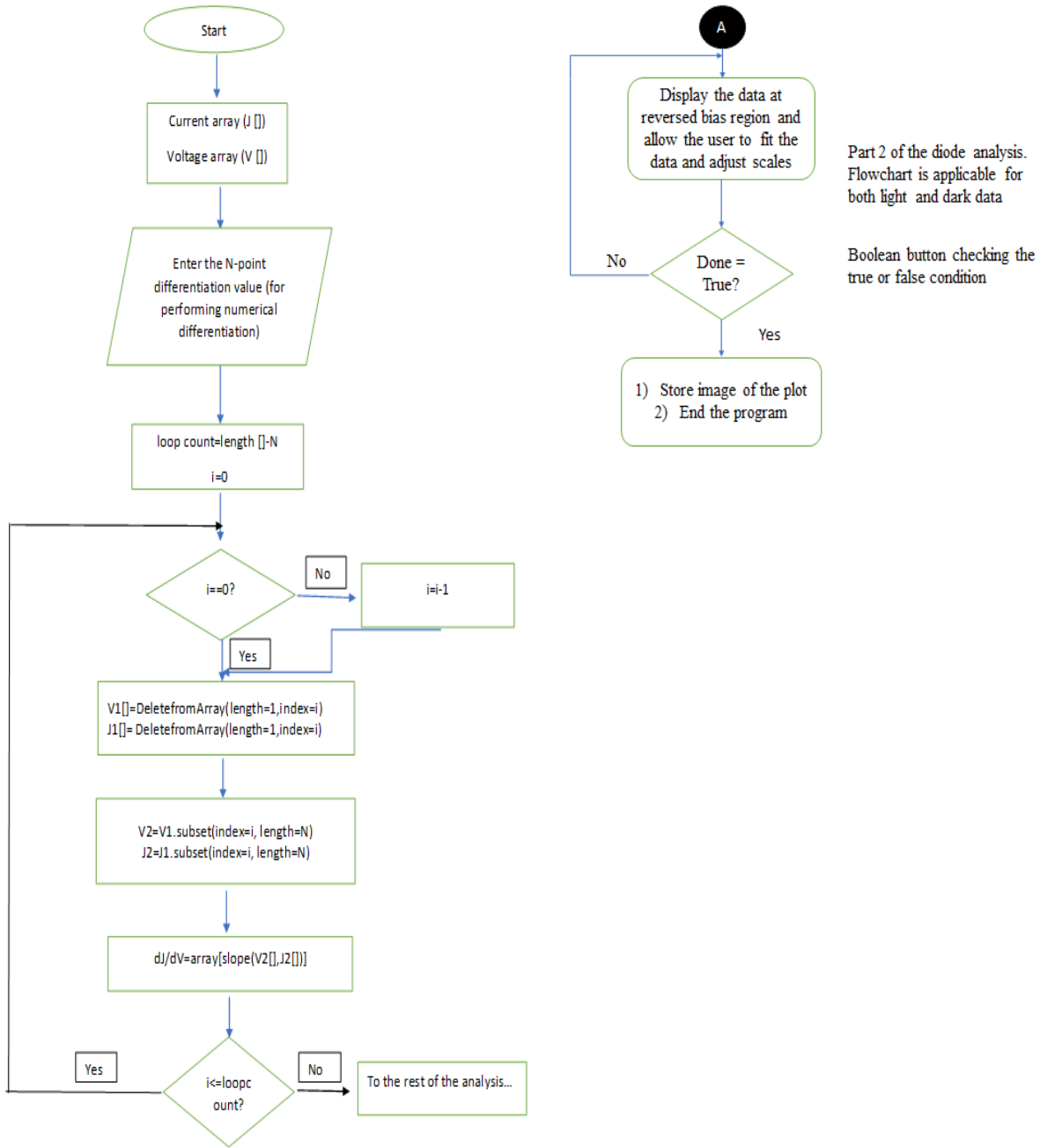


Figure A.1 Flow chart diagram representing the numerical differentiation done in computing the data for dJ/dV under part 2 of diode analysis. Same logic is applied in the 3rd part for computing dV/dJ data.

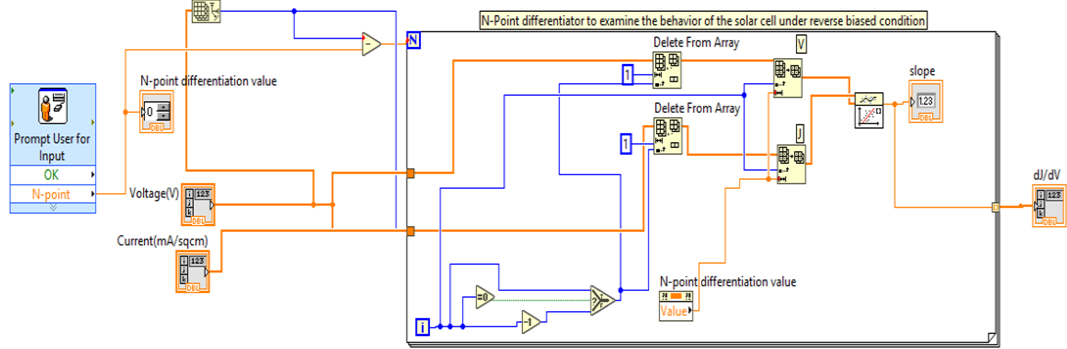


Figure A.2 Block diagram in LabVIEW that performs the numerical differentiation under part 2 of diode analysis.

Appendix B

FILES RELATED TO THE PROGRAM

These are the images related to files generated by the DioMac program. Figure B.1 is the image for the text file that contains the data that has been computed throughout the diode analysis (i.e data computed for dJ/dV , dV/dJ , $V-RJ$, $(J+J_{sc})^{-1}$, $\ln(J+J_{sc}-GV)$) and their respective linear fit data under both light and dark conditions. This data can be helpful for the user to verify the diode analysis of the device using Excel or Origin, or the user can include this data in publications. A text file is created containing the filename, cell ID, type of cell, and ‘analysed@diomac.txt’ extension.

Figure B.2 shows the tabulated results of the diode parameters that gets recorded once the user clicks on the ‘Generate’ button on the program window. The table consists of Filename, cell ID, date and time of execution, the type of solar cell, and other parameters important to understand the solar cell. These results are stored as a record in a text file as shown in Figure B.3.

140716_101321 MC1469-02-001.Silicon analysed@diomac - Notepad

File Edit Format View Help

Current(A/sqcm)	Light	Voltage(V)	Light	dj/dv (mS/sqcm)	Light	dv/dj(ohm sqcm)	Light	$(J+Jsc)^{-1}$ (mA ⁻¹ sqcm)	Light	V-RJ (V)
-0.032166	-0.300072	0.116697	-388.951391	-21.881838	-0.227479	-3.112143	-0.000009	-0.300061		
-0.032166	-0.294298	0.096542	853.686573	-18.903592	-0.221706	-3.151919	-0.000009	-0.294343		
-0.032180	-0.288697	0.043911	361.320754	-17.621145	-0.216073	-3.623606	-0.000009	-0.288692		
-0.032173	-0.282978	0.034358	-408.313867	-22.002200	-0.210368	-3.452485	-0.000009	-0.282973		
-0.032157	-0.277233	0.187200	312.950550	-22.547914	-0.204659	-3.082602	-0.000009	-0.277256		
-0.032171	-0.271639	0.065323	9524.350347	-23.752969	-0.199034	-3.491399	-0.000009	-0.271571		
-0.032153	-0.265943	0.063628	-213.254167	-30.581040	-0.193379	-3.058757	-0.000008	-0.265922		
-0.032152	-0.260229	0.261161	757.097561	-22.522523	-0.187666	-3.082857	-0.000008	-0.260212		
-0.032176	-0.255111	0.076170	1902.833250	-19.120459	-0.182494	-3.897648	-0.000008	-0.254509		
-0.032168	-0.248902	0.070946	-1456.410264	-21.413276	-0.176304	-3.625968	-0.000008	-0.248866		
-0.032165	-0.243194	0.145585	423.925374	-21.208908	-0.170603	-3.578868	-0.000008	-0.243167		
-0.032169	-0.237514	0.016137	3336.233442	-23.584906	-0.164914	-3.803178	-0.000008	-0.237495		
-0.032156	-0.231833	0.083349	3004.000456	-28.694405	-0.159263	-3.381627	-0.000007	-0.231793		
-0.032154	-0.226162	0.060917	-526.250009	-30.257186	-0.153596	-3.381772	-0.000007	-0.226159		
-0.032152	-0.220454	0.311851	-723.230762	-26.666667	-0.147892	-3.376367	-0.000007	-0.220451		
-0.032163	-0.214771	0.244272	348.098159	-21.367521	-0.142184	-3.832157	-0.000007	-0.214747		
-0.032171	-0.209129	0.046431	-508.732145	-23.501763	-0.136526	-4.409026	-0.000007	-0.209116		
-0.032154	-0.203455	0.333260	515.432435	-25.000000	-0.130888	-3.620797	-0.000007	-0.203444		
-0.032166	-0.197758	0.237264	731.181818	-24.968789	-0.125165	-4.279577	-0.000007	-0.197728		
-0.032155	-0.192036	0.054095	-460.419356	-32.626427	-0.119469	-3.762370	-0.000006	-0.192037		
-0.032147	-0.186406	0.124197	897.857133	-30.303030	-0.113856	-3.532350	-0.000006	-0.186398		
-0.032159	-0.180697	0.047670	-525.388886	-27.739251	-0.108119	-4.191745	-0.000006	-0.180695		
-0.032153	-0.175040	0.204107	236.345834	-26.109661	-0.102477	-3.926150	-0.000006	-0.175032		
-0.032164	-0.169366	0.264274	-331.569768	-31.545741	-0.096778	-4.931771	-0.000006	-0.169354		
-0.032140	-0.163694	0.388747	-2113.370061	-35.335689	-0.091160	-3.523075	-0.000006	-0.163678		

Figure B.1 Screenshot of text file containing the calculated data while performing diode analysis.

Tabulated results

Date and time	Voc	Jsc	Fill Factor(%)	Gsh(Light)	Rsh(Light)	Rs(Light)	J0(Light)	Ideality factor(Lig)	Ideality Factor(L
3/21/2019 10:41 P	0.560000	-0.028800	45.200000	4.068878	0.245768	9.303266	8.781044E-1	1.272923	1.697141

Figure B.2 The tabulated results of the diode parameters computed for each sample loaded.

diode parameters results analysed@diomac - Notepad

Filename:	Cell ID	Cell type	Temperature(K)	Date and time	Voc	Jsc	Fill Factor(%)	Gsh(Light)	Rsh(Light)	Rs(L)
141124_120730	MC1455-04-001	.jvtst	MC1455-04-001	FHJ	25.000000	3/22/2012 7:44 AM	0.668300	-0.033810	74.7	
140715_092620	MC1481-03-004	.jvtst	MC1481-03-004	Silicon	26.400000	3/22/2012 7:51 AM	0.580300	-0.033070	70.4	
140715_092620	MC1481-03-004	.jvtst	MC1481-03-004	Silicon	26.400000	3/22/2012 7:51 AM	0.580300	-0.033070	70.4	
140826_102252	MC1492-02-001	.jvtst	MC1492-02-001	Si	25.400000	3/22/2012 7:56 AM	0.676600	-0.037810	72.8	
181109_122245	35727-13-001	.jvtst	35727-13-001	SL/Mo/CuInGaSe2/CdS/ZnO/ITO/Ni-Al grids	25.000000	3/22/2012 8:01 AM	0.628700	-0.034620	0.76	
180123_111805	26015.31-001	.jvtst	26015.31-001	CIS, reg CdS	-105.000000	3/22/2012 8:03 AM	0.456200	-0.036240		
180123_122913	26015.31-001	.jvtst	26015.31-001	CIS, reg CdS	35.000000	3/22/2012 8:06 AM	0.621600	-0.035020		
180123_113324	26015.31-001	.jvtst	26015.31-001	CIS, reg CdS	-75.000000	3/22/2012 8:11 AM				

Figure B.3 Text file that keeps the record of the diode parameters for the samples run by the program